



De-Coupled Moment and Shear Fire Tests

Author: Victor Atkinson

Student number: 388669

Supervisor: Professor Alex Elvin

A research report submitted to the Faculty of Engineering and the Built Environment, University of the Witwatersrand, Johannesburg, in partial fulfilment of the requirements for the degree of Master of Science in Engineering

Johannesburg, 16th September 2021

A handwritten signature in black ink, consisting of several loops and a long horizontal stroke extending to the right.

Table of contents

Abstract	1
1. Introduction	2
2. Decoupled moment and shear: Partial fire testing	3
2.1 Partial fire testing.....	4
3. Furnace development	6
3.1 Objective	6
3.2 Preliminary testing for rationale of the furnace development.....	7
3.3 Dimensions, materials, and construction method.....	8
3.4 Fuel	10
3.4.1 <i>Fuel ignition rationale</i>	10
3.4.2 <i>The final fuel used</i>	11
3.5 Temperature Monitoring and Regulation.....	13
3.6 Loading	15
3.7 Results and Discussion	17
4. Lintel fire tests	24
4.1 Scope	24
4.2 Sample description	25
4.3 Test procedure and monitoring	26
4.4 Results	29
4.5 Discussion	34
5. Conclusion and recommendations for future studies	35
Acknowledgments	36
References	37



List of Figures

Figure 1. Diagram illustrating (a) Arbitrary loading case (b) Ideal loading case and (c) Tested loading case.....	4
Figure 2. Diagram illustrating (a) Load induced plastic hinge and (b) Temperature induced plastic hinge.....	5
Figure 3. Standard fire curve with upper and lower limits as per SANS 10177-2.....	7
Figure 4. Graphical furnace temperature results for tests 3-8.....	8
Figure 5. Illustration of the basic dimensions of the furnace.....	8
Figure 6. Showing (a) Plan view of timber stacked in the furnace, (b) Section A-A and (c) Section B-B.....	11
Figure 7. Photograph taken of the timber arrangement inside the furnace.....	12
Figure 8. Photograph of (a) Lutron TM947SD 4 channel data logger and (b) type K thermocouple.....	14
Figure 9. Illustrating (a) Plan view of the furnace with blowers, (b) Cross section A-A and (c) Cross section B-B.....	14
Figure 10. Thermocouples placed in the centre of quadrants of the furnace lid.....	15
Figure 11. The furnace with loading rig.....	17
Figure 12. Photographs of (a) furnace loading rig and (b) loading rig weights.....	17
Figure 13. Test 9 thermocouple temperatures versus time plot.....	21
Figure 14. Test 10 thermocouple temperatures versus time plot.....	21
Figure 15. Test 11 thermocouple temperatures versus time plot.....	21
Figure 16. Test 9 average thermocouple temperature versus time plot.....	22
Figure 17. Test 10 average thermocouple temperature versus time plot.....	22
Figure 18. Test 11 average thermocouple temperature versus time plot.....	22
Figure 19. Test 9 linearised average temperature versus time plot.....	23
Figure 20. Test 10 linearised average temperature versus time plot.....	23
Figure 21. Test 11 linearised average temperature versus time plot.....	23
Figure 22. Lintel-furnace installation schematic.....	24
Figure 23. Photograph of (a) precast lintel cross section with dimension and (b) without dimensions.....	25
Figure 24. Precast composite masonry lintel fire test specimen schematic.....	26
Figure 25. Photograph of lintel test 1 with no load.....	27
Figure 26. Photograph of lintel test 3 with applied load before ignition.....	28
Figure 27. Photograph of lintel test with applied load during fire test.....	28
Figure 28. Lintel in furnace approximately 24 hours post test.....	30
Figure 29. Lintel fire test 1 photographic results (a), (b), (c), (d), (e), and (f).....	31
Figure 30. Lintel fire test 2 photographic results (a), (b), (c), and (d).....	32
Figure 31. Lintel fire test 3 photographic results (a), (b), (c), (d), (e), (f), (g), and (h).....	34
Figure 32. Cross sections analysed for second moment of inertia.....	35

Abstract

This study investigates the decoupled moment capacity and behaviour of precast masonry lintel beam specimens. The review firstly explores the suitability of partial fire testing to obtain the decoupled moment capacity of beam specimens. Secondly, a low-cost furnace is developed and built that allows for the SANS 10177-2 'standard time temperature curve' to be achieved for 90 minutes. Lastly, fire tests are conducted on three full scale masonry composite concrete lintel specimens by exposing 60% of the clear span about the centre of the element to fire. The best linear regression error between the linearized furnace temperature test results and the standard time temperature curve is calculated to be 3.18% between gradients. It is concluded that the developed furnace can be used to yield the standard time temperature curve and can allow for the testing of horizontal specimens. The results found that fire testing caused delamination between concrete lintels and brickwork and that the specimens no longer behave compositely.

Keywords: fire testing, composite concrete lintel, furnace, standard time temperature curve

A handwritten signature in black ink, consisting of several overlapping loops and a long horizontal stroke extending to the right.

1. Introduction

Fires in buildings are catastrophic phenomena that can have severe detrimental effects. To alleviate these effects, fire engineering and testing has become an integral part of the construction industry by means of codes of practice. To ensure the safety of people and property, codes of practice have been developed to reduce the spread and damage caused by fire. Many forms of standardised fire testing methods have been developed according to a wide range of codes of practice to design better structures and construction materials to withstand the effect of fire.

In South Africa, it is a statutory requirement that structural elements be compliant with the code of practice and that they satisfy the prescribed requirements to withstand exposure to fire for a specific time. This is mainly to allow people time to evacuate and for emergency services to combat the spread of fire. One method of verifying code compliance and building code requirements can be achieved through fire testing.

Compliance can be achieved by adhering to SANS 10400 Part T which satisfies the requirements of the National Building Regulations, issued in terms of the National Building Regulations and Building Standards Act, Act No. 103 of 1977. Under SANS 10400 Part T, fire testing is permitted, and the fire testing verification method is prescribed by SANS 10177:2005 series.

SANS 10177-2:2005 prescribes the method of testing needed to determine the fire resistance of structural elements, based on the length of time within which a representative test specimen of specified dimensions will satisfy the criteria in respect of stability, integrity, and insulation.

SANS 10177-2 clearly defines the requirements that structural elements must adhere to in terms of stability, integrity, and insulation. These requirements are tested qualitatively, predominantly through observation and address the response of an element subject to fire. The prescribed methods make no allowance to further understand or investigate the effect that fire has on internal forces, member capacities and resistances or why the element behaves in a certain way.

This research explores a decoupled moment and shear partial fire testing method that incorporates standard test method procedures for observation and recording. This allows for a better understanding of the contribution that the moment capacity has on the overall fire



rating by exposing the pure bending moment within a centre portion of the beam to the temperatures set out by the standard time temperature curve.

Lintels are used, firstly, as an example to aid the development of the furnace with regards to furnace temperatures, accommodating of structural elements and loading of elements, secondly, to demonstrate and test the concept of partial fire testing. And finally, to investigate the validity of the SANS 1504:2015 assumption of composite behaviour under fire loading.

After conducting a survey on 15 lintel manufacturers throughout South Africa, it transpired that there is some confusion and a lack of clarity regarding South African Bureau of Standards (SABS) approvals. The survey led to the conclusion that no lintel manufacturer has had a fire test conducted on their lintels, thus, there is a high probability that lintels do not have a fire rating because the behaviour of composite masonry lintels subject to fire has not been studied. This indicates that some commercially available lintels might not meet the deemed to satisfy requirements of the code, and subsequently do not adhere to the requirements of the law.

2. Decoupled moment and shear: Partial fire testing

The decoupling of moment from shear is a well-known concept in structural engineering and is based on the mathematical relationship between moment and shear. In brief, for a simply supported beam the relationship can be depicted in the arbitrary loading case (*Figure 1(a)*), when the bending moment diagram, denoted M-Diagram, is at a maximum value the shear force diagram, denoted SF-Diagram, has a minimum corresponding value at the same location along the beam. When referring to the ideal loading case (*Figure 1(b)*), the relationship between moment and shear can be manipulated in such a way as to achieve a pure, constant bending moment over a portion of the beam element, where the contribution of shear has been reduced to a value of zero and its influence completely removed from this portion of the beam element. Over this portion of the beam where shear is zero and moment is at a constant maximum, moment and shear have been decoupled. This manipulation can be very easily achieved through a four-point load test, where the applied load illustrated in *Figure 1(b)* and *(c)* is represented by p in kN. In the ideal loading case where there is only pure bending moment, this is the portion that will be placed in the fire compartment to obtain the decouple moment fire resistance rating for stability. The fire compartment is shown as a dashed line rectangular box in *Figure 1(b)* and *(c)*.



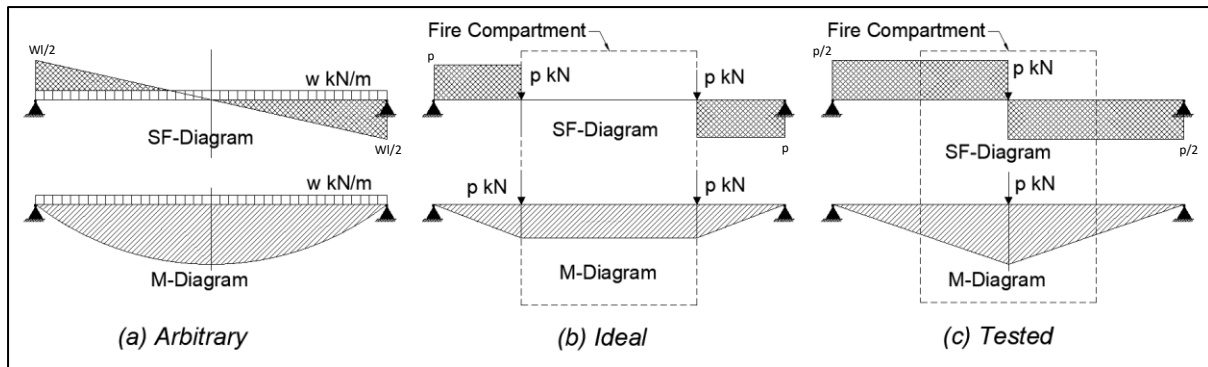


Figure 1. Diagram illustrating (a) Arbitrary loading case (b) Ideal loading case and (c) Tested loading case

The above concept is applied in this study allowing for greater insight into the response of an element to fire loading by joining two forms of standardised testing. However, the loading of the specimens proved challenging and the ideal loading case of a four-point load test has not been achieved. The tested load case in *Figure 1(c)*, of a single point load acting at the centre of the beam is achieved, and a shear contribution remains, thus the moment and shear could not be completely decoupled.

2.1 Partial fire testing

Decoupling the moment and shear forces can allow each aspect to be investigated independently and the effects that fire could have on each aspect. Where the fire compartment depicted in *Figure 1(b) and (c)* does not completely conceal the beam specimen, this is considered a partial fire test. Partial fire testing is conducted on full scale composite masonry lintels acting as beam specimens, where only a 60% portion about the centre of the specimen, is subject to the standard time temperature fire curve and the behaviour of the complete specimen is studied. To test the effects of fire on the moment resistance of the beam element only the portion of the beam that is in pure bending is exposed to fire - not the entire element.

Partial fire testing as opposed to complete fire testing of full scale structural elements can be criticised, however, there are some points listed below that support partial fire testing. Insightful information, predominantly with regards to stability of structural elements, can be gained by only subjecting a portion of the element to fire, which could allow for relationships between partial and complete full-scale fire exposure tests to be determined. It can be considered as a more cost-effective option from which valuable results and understanding can be gained.

Firstly, fires in buildings are unpredictable and complicated to model due to the dependency on many uncontrollable factors. This makes it difficult to predict whether the fire will act on a portion of a structural element or on the whole element.

A great deal of fire engineering design for buildings focuses on disallowing the spread of fire from one compartment to the next. In many cases, particularly in buildings, these compartments are formed and separated by dry walling and partitions. This allows a single structural element to pass through many compartments. This means that if a fire started in one compartment, but is unable to spread to another compartment, the main beam passing through multiple compartments would be partially exposed to fire, in this case, the partial fire test could be related to a compartment fire.

Secondly, with reference to *Figure 2 (a)* of a simply supported beam where collapse of the beam, induced by a load p in kN, is modelled as a mechanism with a plastic hinge forming at the centre of the beam under the load p , indicating that the material has yielded at this position due to the applied load p .

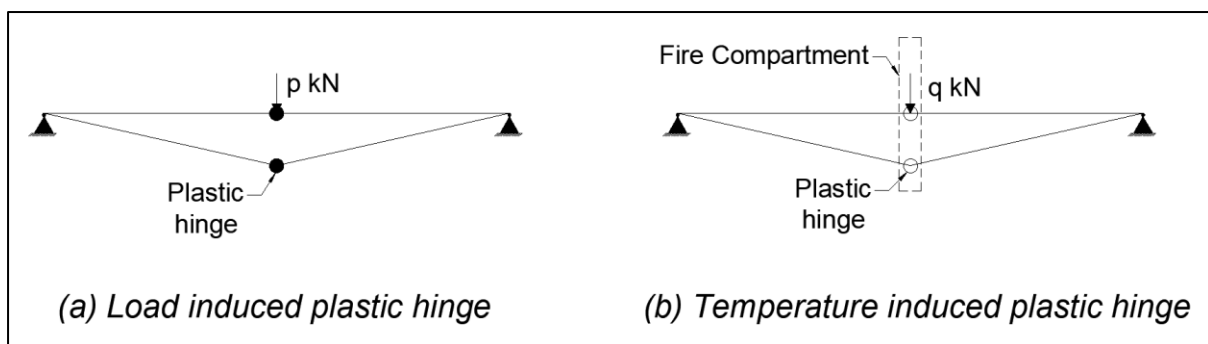


Figure 2. Diagram illustrating (a) Load induced plastic hinge and (b) Temperature induced plastic hinge

With some certainty the position of the plastic hinge can be calculated and predicted indicating where an element or a structure is going to fail by the yielding of the material under normal loading conditions. This yielding of the material happens over a small portion of the beam modelled as a hinge. The yielding in this case is achieved by increasing the load, where the yielding capacities of the material and element are kept constant.

This hinge and mechanism can be achieved in a different way, instead of the load being increased and the material and element properties being kept constant, the loading can be kept constant and high temperature exposure over a small portion of the beam element can be used to reduce the yielding capacity of the material and element causing stability failure or collapse. This would be a temperature induced plastic hinge as shown in *Figure 2(b)* where the fire compartment is shown as a dashed line rectangular box and the applied load denoted q kN.



The small portion of the beam exposed to high temperature would be the portion of the structure or the element that would cause collapse when subjected to fire loading. Partial fire testing in this case is likely to yield identical results to complete fire testing for the fire rating case of stability. One critical aspect that must be considered, when partial fire testing is conducted where the portion being exposed to high temperatures becomes small (*Figure 2(b)*), is that there must be a slice of the cross section that experiences temperatures and temperature gradients throughout the cross-section equivalent to what that slice would experience if the entire beam were subjected to high temperatures.

Another important consideration of fire testing is that the test specimen ought to be tested with identical physical parameters such as loading and boundary conditions as the element would exist in real instances, this is generally referred to as a representative element. It is vital that a representative element is achieved when conducting a fire test, regardless of a complete or partial fire test.

There are also different types and forms of scaled fire testing with associated literature, each with its own set of pros and cons, but literature on partial fire testing of structural elements as it is defined in this study is scarce. Scaled fire testing varies between small-scale and large-scale fire tests, small scale and large-scale elements, small scale in-situ fire tests and laboratory fire tests (Bjorge *et al.*, 2007, Izzuddin & Moore, 2002, Radzi *et al.*, 2006 and Samathipala *et al.*, 2001). Each form of test has its own advantages, disadvantages, and criticisms.

3. Furnace development

3.1 Objective

The first primary objective was to develop a furnace that could produce temperatures with a plot as per the SANS 10177-2 standard time temperature curve (*Figure 3*) with upper and lower temperature limits as illustrated. Temperatures on the curve were calculated with Equation 1 as demonstrated below. The second primary objective was to modify the furnace to allow for fire testing of precast masonry lintels with the option of additional load and no additional load applied to the structural specimen. The secondary objective here was to construct a cost-effective furnace with readily available, off-the-shelf materials, that would be easily operable and scalable.



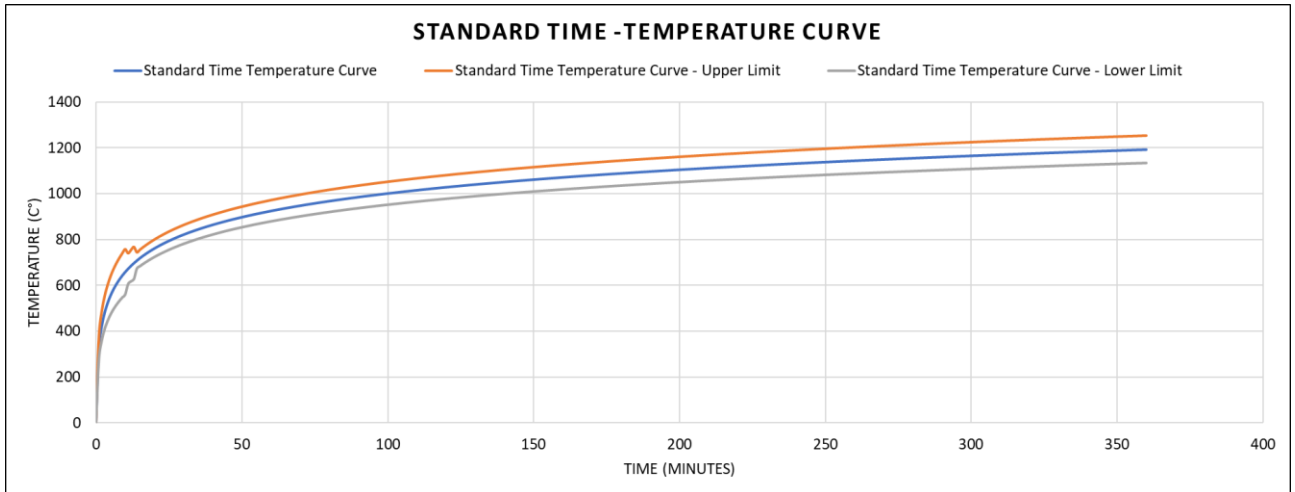


Figure 3. Standard fire curve with upper and lower limits as per SANS 10177-2

Equation 1 below as provided by SANS10177-2 clause 2.2 Standard Heating Conditions:

$$T - T_0 = 345 \log_{10}(8t+1) \dots \dots \dots \text{Equation 1}$$

Where:

t is the time in minutes

T is the furnace temperature at time *t* in degrees Celsius

*T*₀ is the initial furnace temperature in degrees Celsius

3.2 Preliminary testing for rationale of the furnace development

The process of furnace development involved a total of 11 fire tests. Tests 1 and 2 were highly explosive and no test results were recorded. Tests 3 to 8 were predominantly to complete the first primary objective as per section 3.1. Tests 9 to 11 were to study the behaviour of precast masonry lintels with the option of additional load and no additional load applied to the structural specimen. To achieve the temperature plot as per the SANS 10177-2 standard time temperature curve, the development of the furnace was a continual improvement process. The furnace dimensions, materials, construction method, the fuel, temperature monitoring and regulation were all elements that needed to be refined to achieve acceptable results.

Figure 4 below represent the graphical temperature results for tests 3-8 assigned to the first primary objective. Tests 9, 10 and 11 were precast masonry lintel fire tests. The furnace temperature results from the last three tests are split and individually analysed for the correlation between the test results and the standard fire curve and discussed in greater detail in section 3.6.

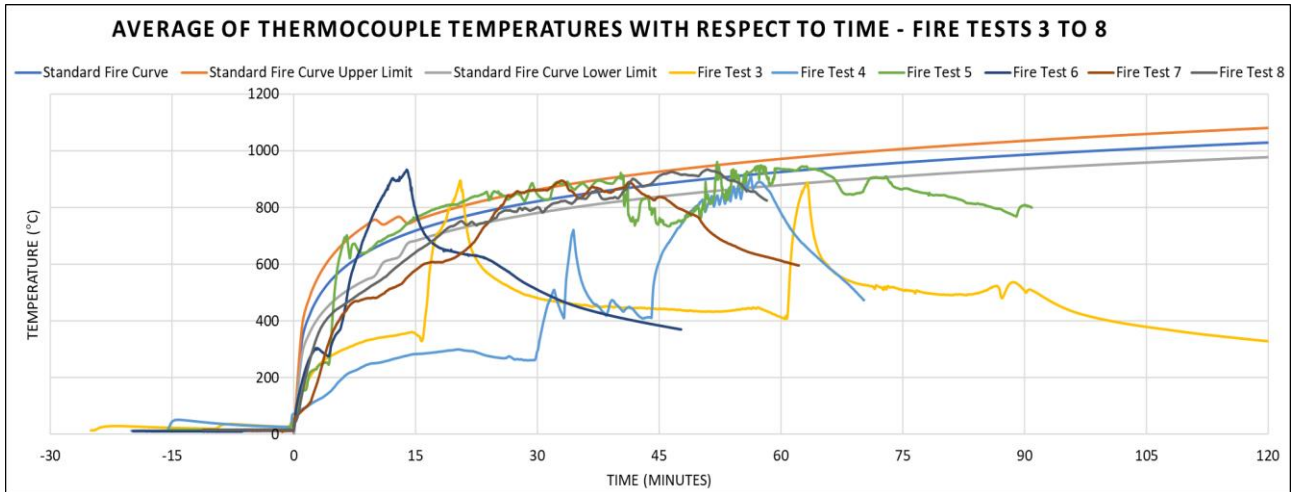


Figure 4. Graphical furnace temperature results for tests 3-8

3.3 Dimensions, materials, and construction method

The final dimensions of the furnace were selected considering three aspects; the first aspect considered the scalability of the furnace with the initial internal dimensions chosen as 1m by 1m in plan - making it one by one reduces certain complexities. A 1m-by-1m furnace was used for tests 1 to 8. The second aspect considered the length of the furnace where the width had been finalised as 1m. The length had an upper limit of 2m established by the clear spacing of a standard 2.4m precast concrete lintel, discussed in section 4, the lower limit of 1m as discussed above. A scaling factor for the length of 1.2m was arbitrarily chosen which demonstrated scalability by 20% and coincided with a 60% fire tested length of 1.2m. The third aspect, the height, considered the space required by the height of the composite masonry lintel, the height required by the fuel and the height required by the air system. From all the aspects considered, the final furnace had overall internal dimensions of 1000mm width, 1200mm length and 1700mm in height as shown in Figure 5.

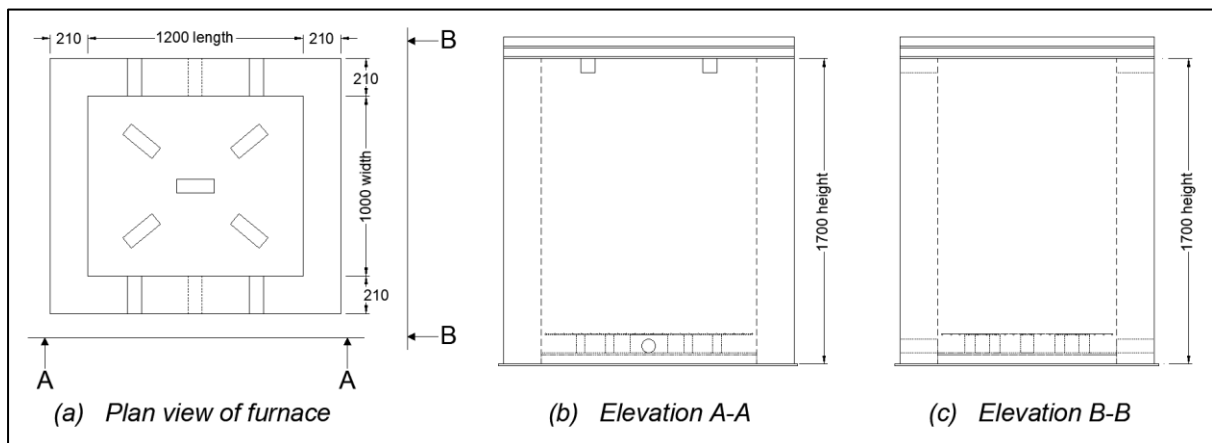


Figure 5. Illustration of the basic dimensions of the furnace



The main furnace enclosure was constructed with a double masonry skin approximately 210mm thick. The double masonry skin was constructed with standard, off-the-shelf 7MPa cement stock bricks¹ that are 222mm in length, 106mm in width, and 73mm in height and with mortar having a cement-building sand mix ratio of 1:3.2 PPC OPC CEM I 52.5N² to building sand. Double skin brick-force with 2.5mm wire thickness and dimensions of 150mm by 290mm, was installed between each course of bricks.

The furnace was double leaf all round with no intentional focus on the air gap between the two skins of brick work, however, if an air gap were maintained throughout it would increase the insulation of the side walls of the furnace and the durability. The two skins were only tied together by brick-force.

For insulation at the base of the furnace, the entire furnace was constructed on top of a 12mm thick fire board³. On top of this fire board on the inside of the furnace a layer of ceramic fibre board 50mm thick was installed, with an additional 12mm thick fire board placed on top of the ceramic fibre board for protection.

At the bottom inside the furnace bricks were placed for two reasons. The first reason was to create an air void to allow for free air movement within the void, and secondly, to allow for free air movement from the void at the bottom of the furnace to the top of the furnace where the exhausts were located. The bricks were oriented in such a way as to direct air to the cold spots within the void of the furnace. The bricks allow the air holes for the air pipes from the blowers to fit into the void, refer to section 3.5 for air regulation. The furnace had four exhausts at the top level with two exhausts on either side, and on the same sides as the air hole inlets for the air pipe from the blowers.

The bricks were additionally used to raise and carry the fuel, refer to section 3.4 for fuel used. A steel mesh grid⁴ with 3.75mm diameter strands and square spacing of 50mm was placed between the bricks and the fuel to help balance the fuel on the bricks.

The lid was constructed using a steel frame to which fibre boards⁵ (dimensions 500mm by 1000mm) were fastened with ordinary 6mm galvanised steel bolts. The steel frame was used as the fixing structure, due to the susceptibility to damage of the ceramic fibre board, especially after exposure to high furnace temperatures.

¹ Purchased from Builders Warehouse Strubens Valley, manufacturer unknown.

² PPC cement supplied by the Wits School of Civil and Environmental engineering.

³ Manufacturer unknown, supplied by Professor Alex Elvin.

⁴ Purchased from NJR Steel Westdene.

⁵ Purchased from RMS, Resistant Materials Services, Boksburg.



A first layer of ceramic fibre blanket was placed between the steel frame and the ceramic fibre board to further insulate and seal any gaps between the ceramic fibre boards and to increase the insulation of the steel.

For thermal insulation and sealing between the top perimeter of the furnace and the underside of the lid a second layer of ceramic fibre blanket⁶ 50mm thick 200mm wide was placed. This was to create a snug fit between the lid and the furnace.

3.4 Fuel

A choice of fuel for the furnace had to be made between liquified petroleum gas (LPG) and timber. Timber was chosen on the merit of cost, but even though LPG might be more expensive it is a far less limited than timber.

3.4.1 Fuel ignition rationale

From tests 1 to 8 conducted, it was found that the initial portion of the fire curve associated with the ignition and rapid heating was dependant on the liquid fuel type used and on surface area of timber⁷, i.e., the greater the surface area that ignites and the rate at which the surface area ignites, the faster the initial rise in temperature. The duration of the fire curve is dependent on the cross-sectional area of the timber used i.e., the larger the cross section of timber the longer the duration of the fire test. The aspects that control the initial portion of the curve and the duration are dependent, and a compromise must be made. The effect of moisture content of the timber was observed, influencing the duration of the fire test i.e., the greater the moisture content the greater the duration of the fire test. The overall amount of fuel in the furnace would affect both the initial temperature and duration of the fire.

Test 1 conducted with only thinners as the liquid fuel type for ignition and test 2 conducted with a mixture of thinners and turpentine as the liquid fuel type for ignition, were highly explosive due to the volatility of the thinners resulting in a build-up of vapour causing a rapid reaction, creating pressure in the confined space of the furnace, which has only a few small openings. This explosion caused the lid to blow off.

After the explosions, sunflower oil was used as the liquid fuel type for tests 3 to 5, however sunflower oil does not allow for the rapid increase in temperature for the initial part of the curve.

⁶ Purchased from RMS, Resistant Materials Services, Boksburg.

⁷ Sponsored by TimRite.



After test 5 and for all the subsequent tests, diesel was used as the liquid fuel type for ignition, even though the initial portion of the curve was not perfected.

Furnace ignition of all the fire tests was challenging. For this reason, it is suggested that a fuel mixture of diesel and turpentine be attempted. Turpentine is miscible in diesel whereas thinners is not, for this reason the mixture might not be explosive and might yield the desired initial temperatures required. The turpentine would allow all the fuel within the furnace to ignite at a faster rate. It is proposed that a mixture is developed such as a 2:8 turpentine to diesel.

Two methods of igniting the furnace were attempted. The first method was a string dipped in thinners and pulled through the furnace, then lit externally. The most effective method of igniting the furnace was with an extended Bunsen burner type flame connected to an LPG gas bottle.

3.4.2 The final fuel used

The main bulk source of fuel used for the furnace was wood which was predominantly responsible for the duration of a fire test. The timber used was square eucalyptus poles with cross-sectional dimensions of 100mm by 100mm, and with lengths of 950mm and 1150mm corresponding to 50mm less than the plan dimensions of the furnace as shown in *Figure 6(a), (b) and (c)*. The 50mm shortening was to create tolerance for ease of placement of the timber in the furnace. The timber was placed into the furnace in a configuration as shown in *Figure 6(a), (b) and (c)*.

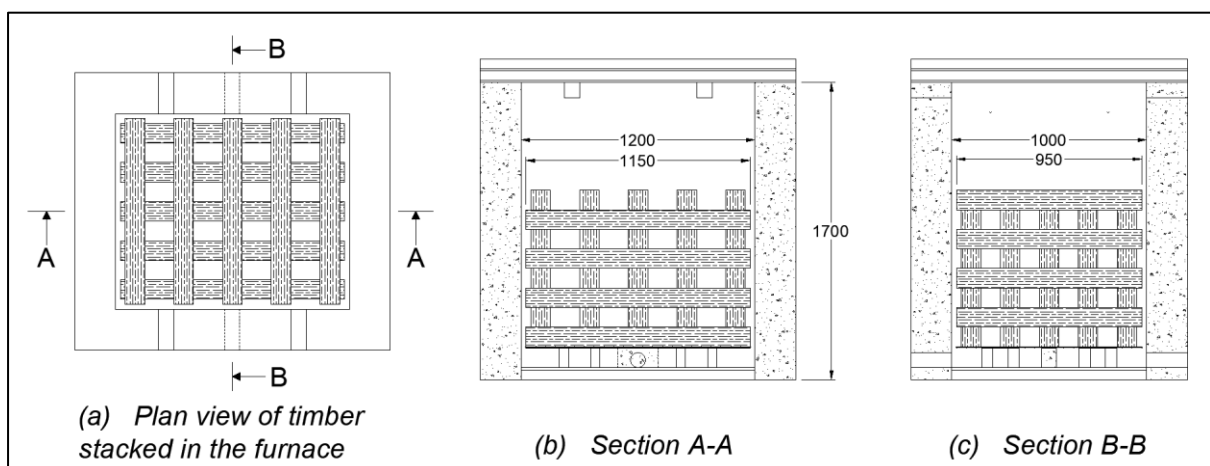


Figure 6. Showing (a) Plan view of timber stacked in the furnace, (b) Section A-A and (c) Section B-B

The furnace was designed in such a way that the fuel gets preloaded into the furnace, *Figure 7*, and that no additional fuel can be added to the furnace during a fire test. This design produces a fixed duration of testing for approximately 90 minutes. The furnace is loaded with a finite amount of fuel for each fire test, determined and limited by the availability of space within the furnace making the furnace a “finite fuel furnace”. This is of course a limitation of the furnace, that the amount of fuel is dependent on the overall height of the furnace, i.e., if the duration of a test were to be increased, the height of the furnace would have to be increased to allow for more fuel.

The total amount of timber loaded into the furnace for each test had an average mass of 280kg, an average density of 668 kg/m³ and a calculated exposed surface area of approximately 14.1m². A total of 40 poles are used for each test.

Prior to the timber being placed inside the furnace, the timber was completely submerged in diesel⁸ for approximately 10 minutes. This additional fluid form of fuel was to allow for rapid ignition of the timber surface to simulate flashover and was responsible for the initial portion of the standard fire curve.



Figure 7. Photograph taken of the timber arrangement inside the furnace

⁸ Diesel 50ppm, purchased from Campus Motors, Westdene

A handwritten signature in black ink, consisting of several loops and a long horizontal stroke extending to the right.

3.5 Temperature Monitoring and Regulation

The furnace temperatures were monitored and recorded with a four channel Lutron TM947SD data logger (*Figure 8(a)*). The furnace temperatures were measured using four type k thermocouples probes⁹ (*Figure 8(b)*) denoted K1, K2, K3 and K4 in *Figure 9 (a), (b) and (c)*. A thermocouple was placed in the centre of each quadrant of the lid at the top level of the furnace as shown in *Figure 9* and *Figure 10*. Each thermocouple was connected to the data logger with a 3m long extension cable¹⁰ in a heat resistant sheath. Temperature values for each of the four type k thermocouple probes were recorded every two seconds for the entire duration of the fire test.

The temperature of the furnace was continuously and manually monitored and compared to the theoretical value of the standard time temperature curve for every respective 1-minute interval. Depending on whether the furnace temperature was above or below the theoretical value as stipulated by the standard time temperature curve, the furnace temperature was adjusted accordingly to either increase or decrease the temperature of the furnace

The temperature in the furnace was adjusted by regulating the amount of air pumped into the furnace. To pump air and oxygen into the furnace two electrical STIHL BGE 71 blowers were used, each with a capacity of 670m³/h as illustrated in *Figure 9(a)*. Adjustment and control of the furnace temperature was done manually by means of two gate valves¹¹, one connected to each blower. The two gate valves were connected to each other so that that the blowers worked together in unison, to not create an imbalance of air inflow into the furnace. To decrease the temperature of the furnace, the gates of the valves were pushed down simultaneously by the same amount to close and decrease the air flow. To increase the temperature of the furnace, the gates were pulled up to open and increase the air flow. The furnace temperatures are highly dependent to the size of the adjustments made to the gate valves and the effects of opening and closing were meticulously observed.

The design intention is to maximize the distance that the air must travel from the inlets of the furnace which are at the bottom of the furnace to the exhausts which are at the top of the furnace. The two air inlets are placed directly opposite each other, to increase the turbulence of air within the furnace and thus adding to the distance the air must travel to the exhaust.

The turbulence and traveling distance increase the contact area of the air which increases the rate of the reaction which results in higher temperatures being produced.

⁹ Purchased from Thermocouple Products (Pty) Ltd, Edenvale

¹⁰ Purchased from Swift Heat & Control, Aeroton.

¹¹ Purchased from APVF, African Pipes Valves & Fittings, Edenvale.





Figure 8. Photograph of (a) Lutron TM947SD 4 channel data logger and (b) type K thermocouple

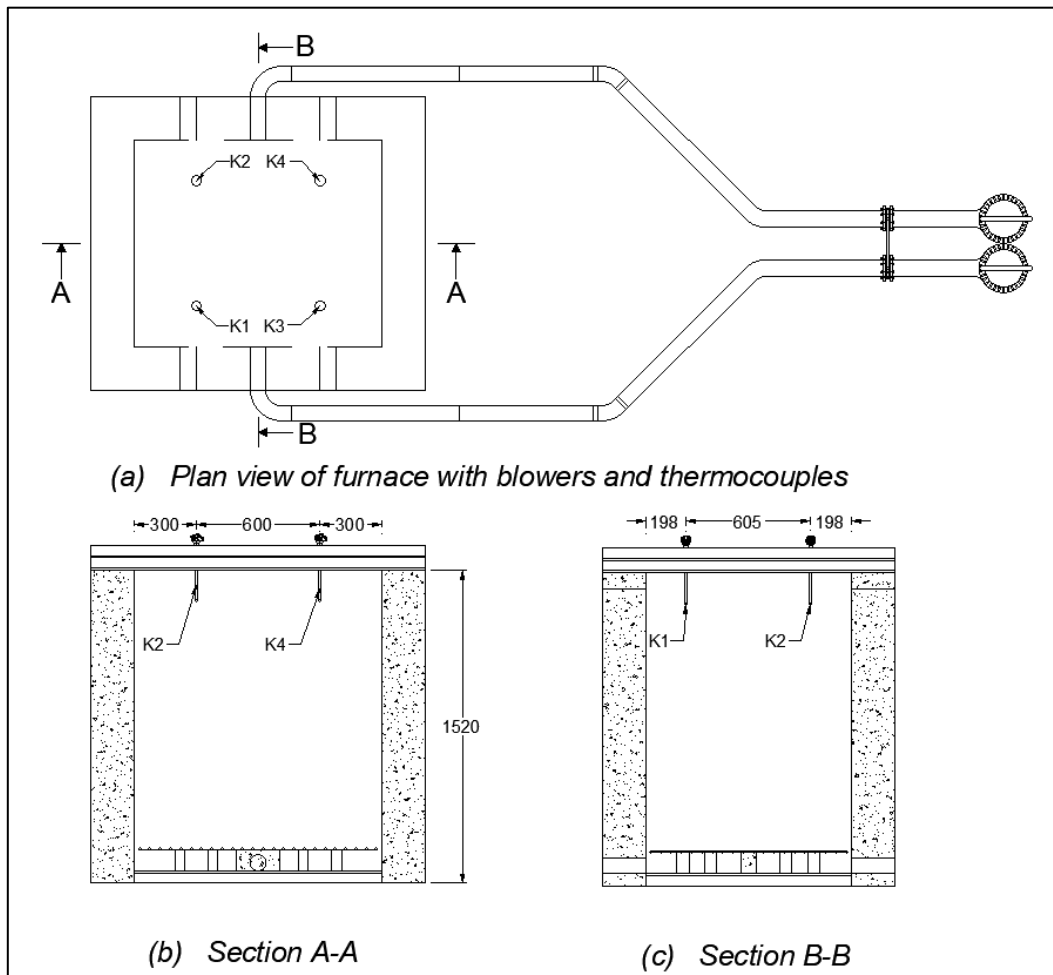


Figure 9. Illustrating (a) Plan view of the furnace with blowers, (b) Cross section A-A and (c) Cross section B-B

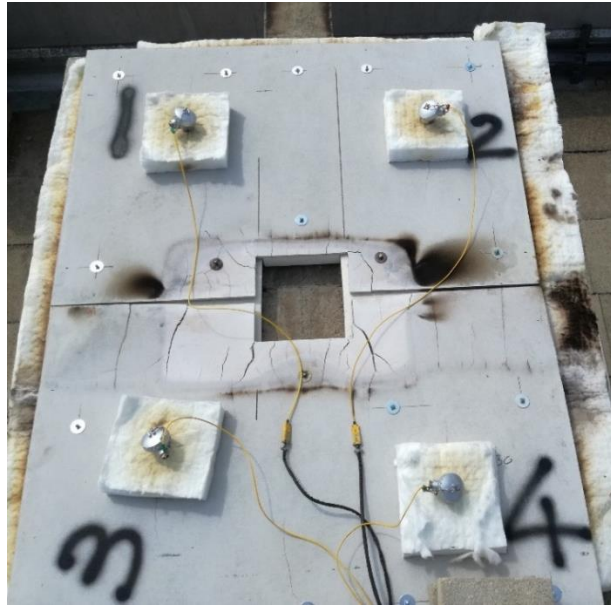


Figure 10. Thermocouples placed in the centre of quadrants of the furnace lid

3.6 Loading

The additional externally applied loading of the specimen was done using a loading rig that is similar in concept to a balancing scale with the balancing weights on either side being identical in magnitude, see *Figure 11* and *Figure 12(a)*. The main difference in concept between the balancing scale and the loading rig is the addition of sliders that prohibit rotation of the central beam about the “central knife edge” or central pin in two directions, in plane and out of plane. These sliders do however allow for vertical movement of the load rig and therefore the transfer of a vertical load through the central pillar to the specimen being tested causing the specimen to deflect vertically.

The central pillar responsible for transferring the vertical point load was constructed with reinforced concrete with cross sectional dimensions of 220mm by 220mm and a height of 300mm. The concrete pillar was placed unfastened to the test specimen at the bottom. At the top of the concrete pillar, the concrete pillar was bolted to a steel base plate with four threaded 10mm diameter anchor bolts. The anchor bolts were cast into the concrete pillar, with an embedment length of approximately 250mm and with an anchor washer and two nuts on the ends.

The steel base plate, 8mm thick with plan dimensions of 220 mm by 220mm was welded to the centre of the horizontal central beam, forming a double cantilever.



The central beam was made up of two square steel tubes¹² welded together, each tube having dimensions of 80mm by 80mm and a wall thickness of 6mm. The total length of the central beam was 2200mm.

On either end of the central beam, 80mm in from the edge a 20mm I-nut¹³ was bolted to the underside of the beam. A lever hoist¹⁴ was hooked through the I-nut with the top hook (*Figure 11* and *Figure 12(a)*). The bottom hook of the lever hoist was connected to a 16mm I-nut on each corner of a steel frame with 10mm D shackles, 8mm mallions and an 8mm chain.

The steel frame acted as a pan to hold the weights that create the externally applied load, *Figure 12(b)*. The total weight in each pan, on either side of the central beam was 3.14kN, creating a total externally applied point load of 6.28kN. The weight in each pan was created using 16, 1.2m lintels¹⁵ each with a weight of 0.2kN stacked in the rectangular steel frame. The lintels were stacked in four layers consisting of four columns, between each layer a 5mm rubber strip was placed to stabilise the stacked lintels.

The horizontal steel central beam was connected on either side to the two vertical sliders which were bolted to the exterior of the furnace. The vertical sliders consisted of two components; the sliding poles made of solid 20mm by 20mm steel bar spaced approximately 85mm apart and bolted to the furnace and the square hollow tubes that were welded to the steel beam and had the poles passing through them.

The load was raised approximately 60mm off the ground by jacking the lever of the lever hoists on either side simultaneously. This meant that the test specimen could deflect 60mm vertically before the load no longer acted on the test specimen.



¹² Purchased from King Steel, Wadeville.

¹³ Purchased from President Bolt, Fordsburg.

¹⁴ Sponsored by Height Safety, Midrand.

¹⁵ Sponsored by CIK Concrete, Boksburg.

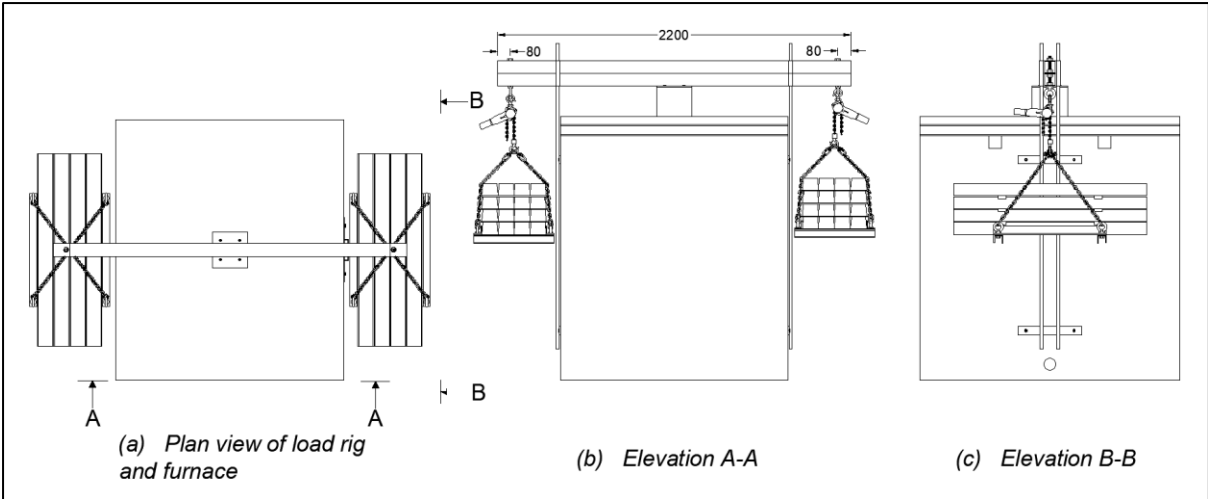


Figure 11. The furnace with loading rig



Figure 12. Photographs of (a) furnace loading rig and (b) loading rig weights

3.7 Results and Discussion

It was observed after tests 1 to 8 and tests 9 to 11, that the major deterioration of the furnaces was cracking, most likely due to thermal expansion of the bricks of the inner leaf exerting a force on to the outer leaf especially where mortar had filled the airgap between the two courses of brick.

Referring to *Figure 13, 14 and 15*, corresponding to the recorded temperature results of tests 9, 10 and 11 and showing the recorded temperatures plotted against the standard temperature curve with upper and lower limits. Temperatures in degrees Celsius are plotted on the y axis and the corresponding time in minutes is plotted on the x axis. For the analysis and comparison, the test results are shifted so that the start of the test is evaluated from time 0. This shift allows for the start of fire test and the standard fire curve to both be at 0. The zero-value on the test results was determined by taking a best fit, where most of the data follows the standard fire curve. A test is concluded once the recorded furnace temperature falls below the lower limit, indicating that the required temperatures cannot be reached regardless of how much air is being pumped in.

The plots can be broken up into three distinct stages, namely, the first stage indicating ignition of the furnace, the initial stage, indicating rapid temperature increase where the blowers are switched from on to off and the duration stage of the test where the blowers are regulated.

The ignition stage of the curve shown by the recorded furnace temperature values from the actual start of the test to just before 0 with a corresponding temperature value of approximately 200 degrees Celsius. From this portion of the curve in each test indicating ignition was an issue with the diesel not easily igniting. During the ignition stage the blowers are turned off completely and only turned on once the diesel ignited, and the temperature has reached approximately 200 degrees Celsius. The rise in temperature for the ignition stage is dependent on the rate at which the diesel on the timber surface ignites which in turn is dependent on many aspects. As it can be seen, the ignition temperatures do not rise fast enough. The problem encountered during ignition can be resolved by dipping the timber in a faster igniting fuel such as a mixture of diesel and turpentine.

The initial stage starting at approximately 200 degrees Celsius, where a steady increase in temperature can be observed and where the blowers are still turned on and valves completely open and ending at the first big dip in recorded furnace temperatures, indicate the start of the temperature regulation as per standard time temperature curve.

There is a very turbulent overlap between the ignition stage and the initial stage. This transition is intended to be smooth, but a clear jump can be seen where the blower is first turned on showing a slight dip as cold air comes in and then an increase at around 200 degrees where the fire is consuming fuel.



The duration stage of the curve corresponds to the first dip in the curves at approximately 700 degrees all the way through to the end of each test. This stage of smooth temperature regulation can be clearly seen by the constant peaks and troughs indicating where the gate valves of the blowers were gently opened and closed little by little. The durations of tests 9, 10 and 11 are approximately 113 minutes, 91 minutes, and 102 minutes, respectively with an average of 102 minutes for all 3 tests.

From the figures, there was a slight difference in temperature on opposite sides of the furnace with thermocouples 1 and 3 both higher in test 9 and then both lower than thermocouples 2 and 4 in tests 10 and 11, which is most likely due to a difference in the contribution of air from each blower, possibly from a difference in adjustment of the gate valves.

Figure 13, 14 and 15 indicate that the general shape of the results fits the standard fire curve and its limits rather well.

Referring to Figure 16, 17 and 18, showing the average temperature values of the four thermocouples for the furnace against time. The average temperature seldom drops below the lower limit or rises above the upper limit.

The moving average shown in green on Figure 16, 17 and 18 is conducted for the portion of the plots where the temperature is regulated. The starting point for analysis of the moving average is taken from the first peak, indicating that temperature regulation had begun, an interval of 120 data points equating to 4 minutes, which roughly included two peaks and two troughs was used for the moving average analysis.

Figure 19, 20 and 21 show the linearised values and plots of the average furnace temperature, the linearised values and plots of the standard time temperature curve with its corresponding upper and lower limits, and the linearised values and plots of the moving average. Equation 2 below is Equation 1 linearized and in the form $y = mx + c$, where the y value corresponds to $10^{(T-T_0/345)}$, m the gradient with a value of 8, x corresponding to t which is time in minutes and c the y intercept with a value of 1. Equation 2 as shown below was used to linearise the average temperature plots, with all y intercepts being set equal to 1.

$$10^{\left(\frac{T-T_0}{345}\right)} = 8t + 1 \dots \dots \dots \text{Equation 2}$$

Where:

t is the time in minutes

T is the furnace temperature at time *t* in degrees Celsius

T₀ is the initial furnace temperature in degrees Celsius



From the linearised plots, a linear least square fit for the data was calculated to be 0.96, 0.90 and 0.97 for tests 9, 10 and 11, respectively. The fit is calculated from the raw data and the best fit straight line drawn through the data. The gradient error between the best fit line and the standard time temperature curve was calculated to be 4.68%, 12.41% and 3.18% for tests 9, 10 and 11, respectively.

To gain a complete understanding of how well the recorded temperatures of test 9 10 and 11 matched the standard time temperature curve, the portions where the recorded temperatures fall beyond the limits, must be quantified in terms of duration and severity.

A handwritten signature in black ink, consisting of several overlapping loops and a long horizontal stroke extending to the right.

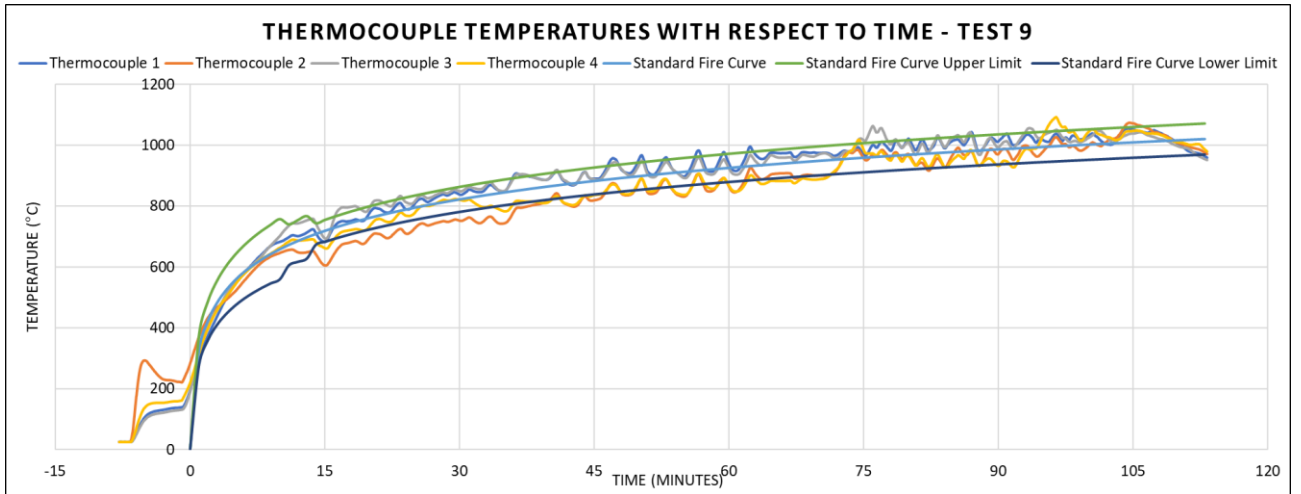


Figure 13. Test 9 thermocouple temperatures versus time plot

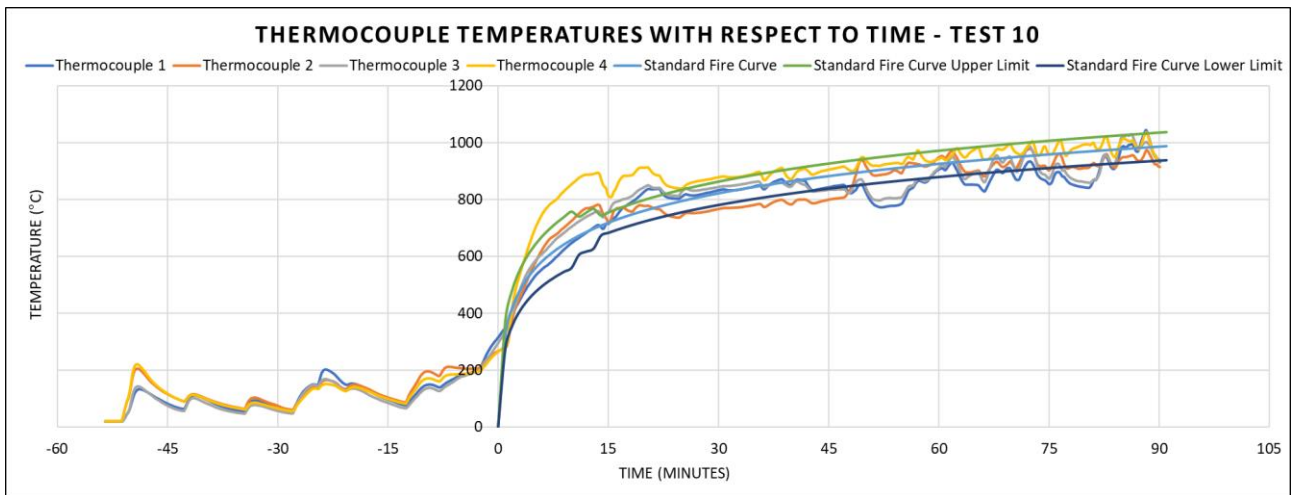


Figure 14. Test 10 thermocouple temperatures versus time plot

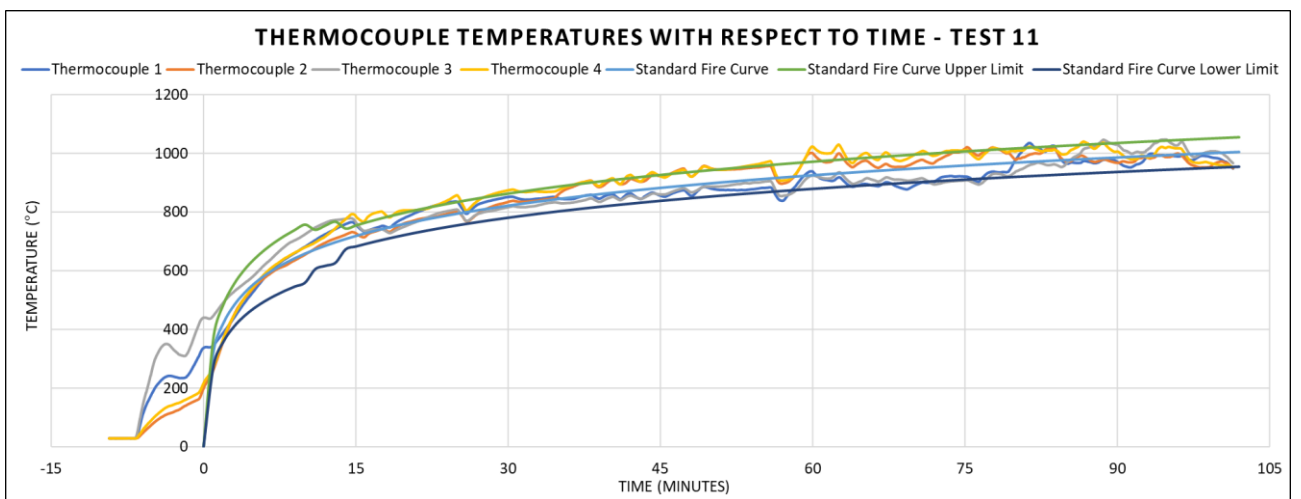


Figure 15. Test 11 thermocouple temperatures versus time plot

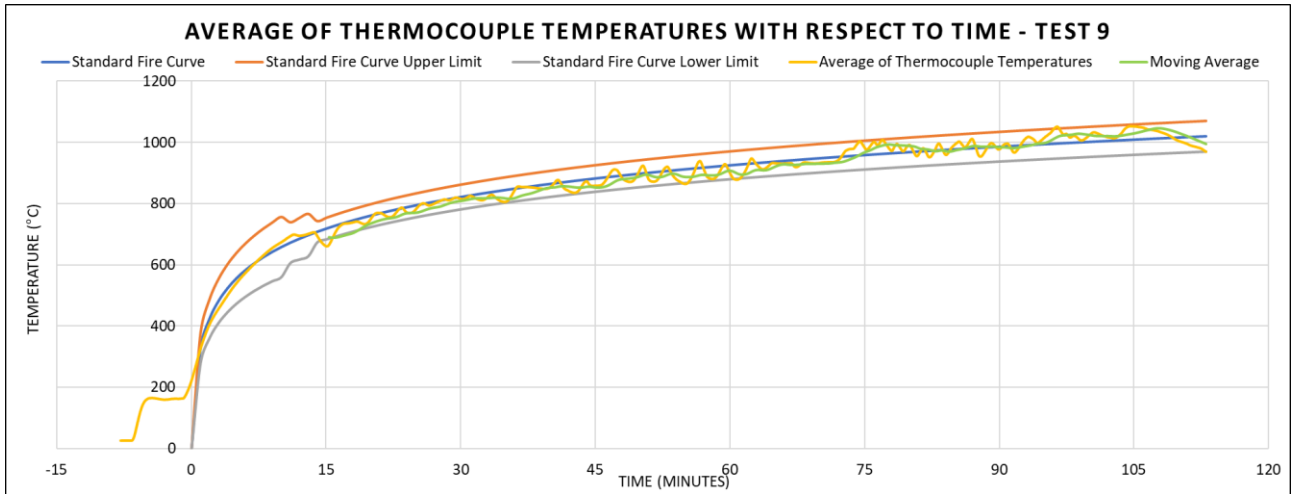


Figure 16. Test 9 average thermocouple temperature versus time plot

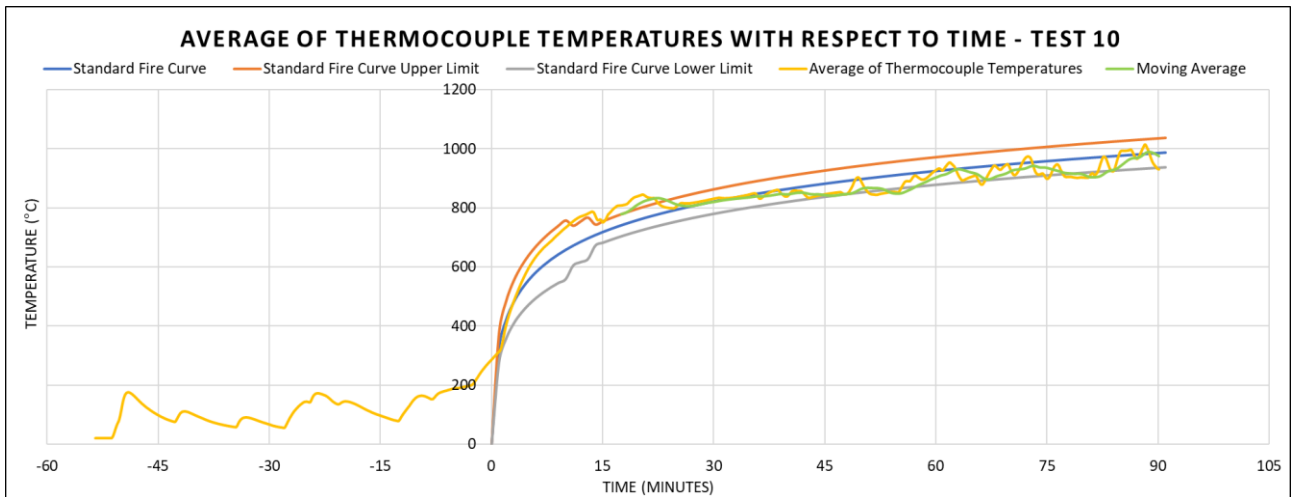


Figure 17. Test 10 average thermocouple temperature versus time plot

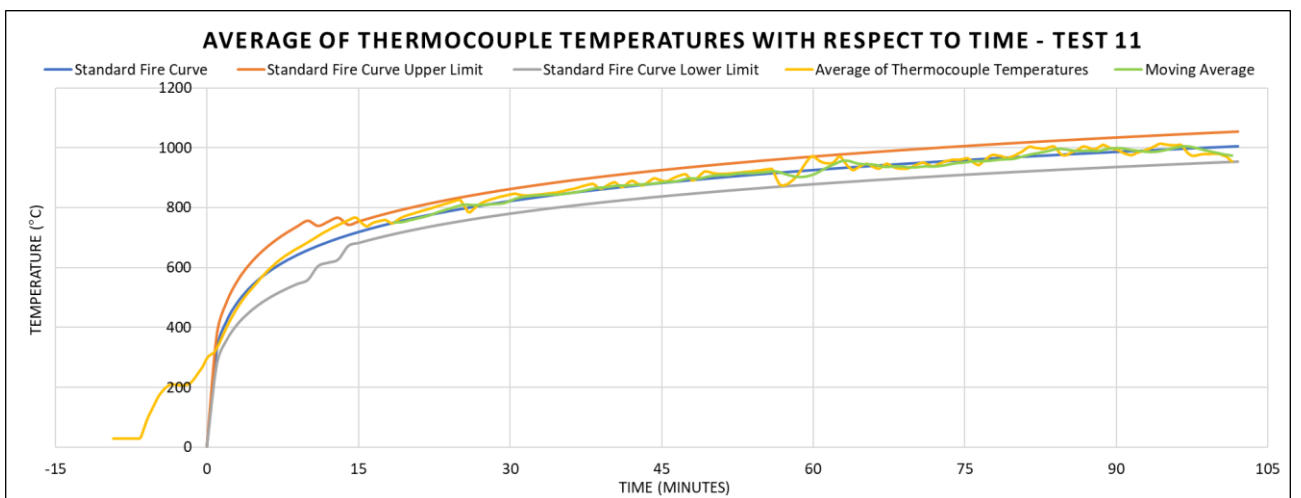


Figure 18. Test 11 average thermocouple temperature versus time plot

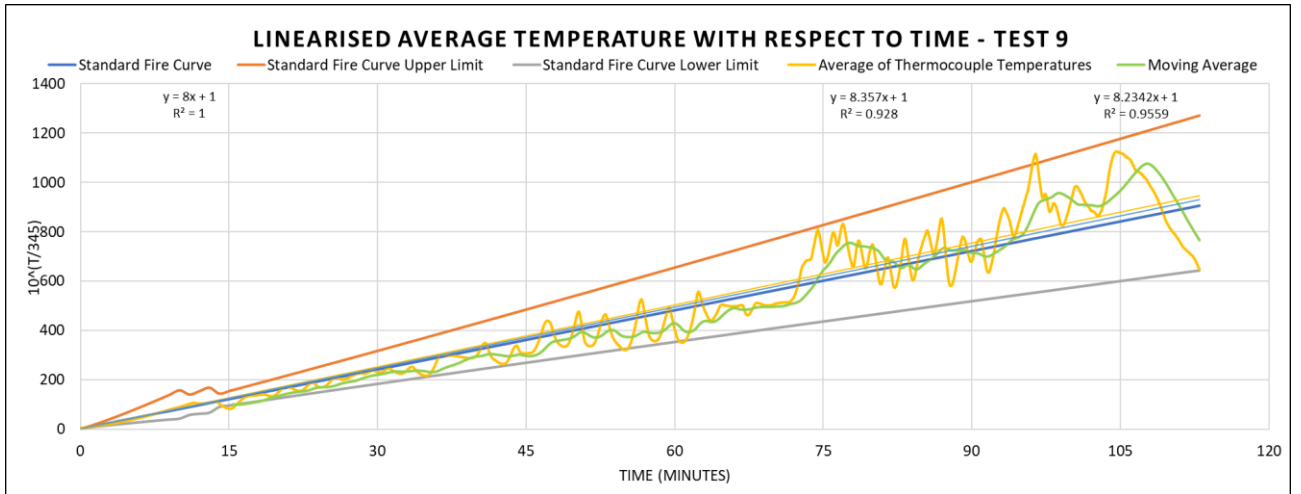


Figure 19. Test 9 linearised average temperature versus time plot

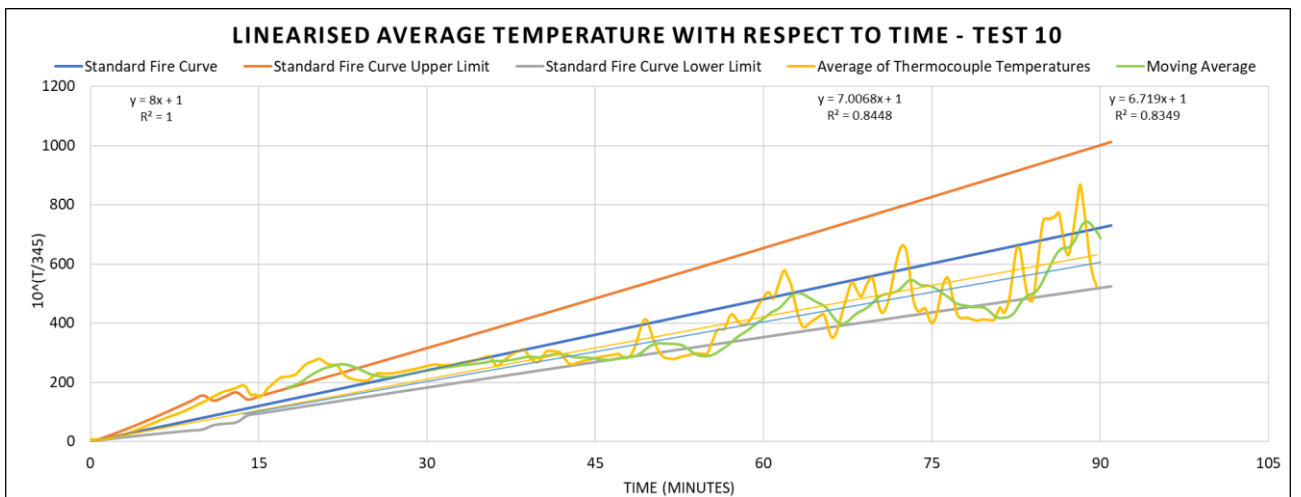


Figure 20. Test 10 linearised average temperature versus time plot

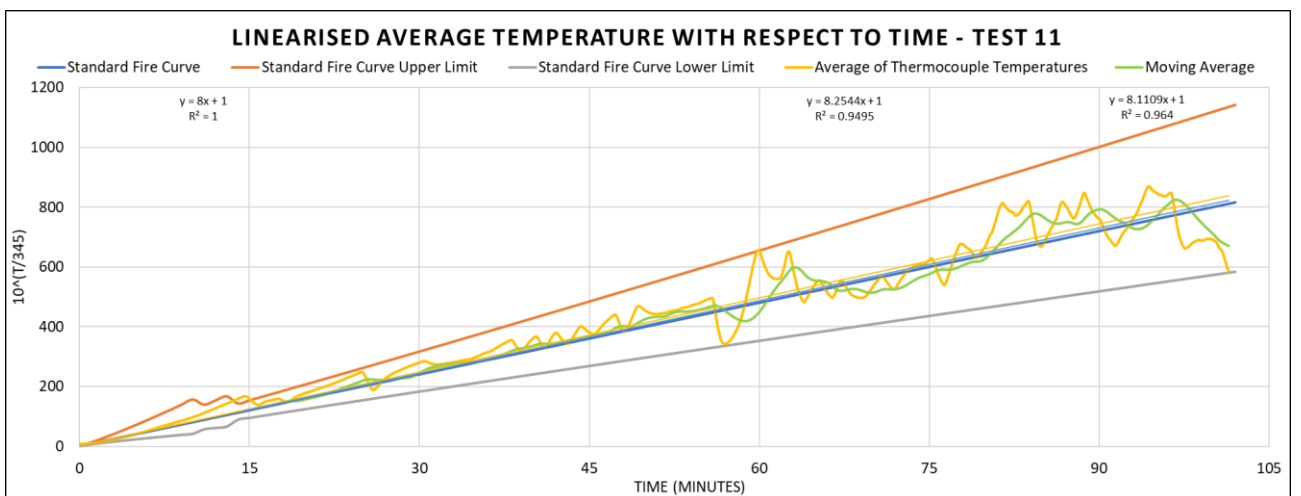


Figure 21. Test 11 linearised average temperature versus time plot



4. Lintel fire tests

4.1 Scope

This section studies and evaluates the behaviour and fire rating of composite concrete lintels using the SANS10177-2 test protocol as a guide. A total of three composite lintel specimens were fire tested with each specimen being installed in the previously developed furnace as a simply supported composite beam with a clear span of two meters using SANS 10164 as a construction and installation guide. *Figure 22* illustrates the composite masonry lintel installed in the furnace. All three of the composite lintel specimens were un-plastered. The first two test specimens corresponding to test 9 and 10 from section 3 had no additional external load applied to them other than their own weight, test specimen 3 corresponding to test 11 from section 3 had an additional external point load of 6.28 kN applied at the centre of the specimen. The test specimens were exposed to fire on 3 sides, left side, right side and bottom, the top of the specimen was not exposed to fire. Only 60% of each specimen about the span centre was exposed to fire.

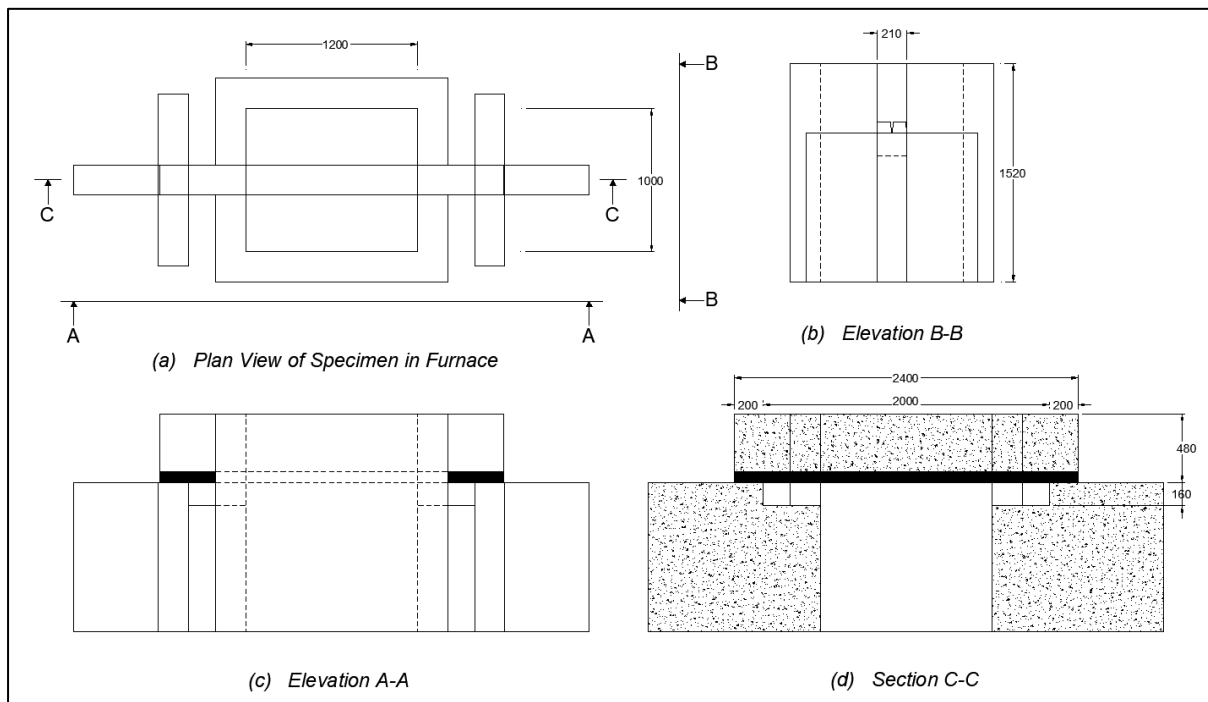


Figure 22. Lintel-furnace installation schematic

4.2 Sample description

The lintels¹⁶ used to form the precast masonry lintel fire test specimen were precast and pre-stressed concrete lintels of 75mm height, 100mm width, and overall length of 2.4m not manufactured in accordance with SANS 1504. Each lintel had five pre-tensioned 2.64mm diameter high tensile carbon steel wire strands which were lightly crimped. Cover to the tendons ranged from 15mm to 20mm. A cross section of the lintel is shown below in *Figure 23(a)* and *(b)*.

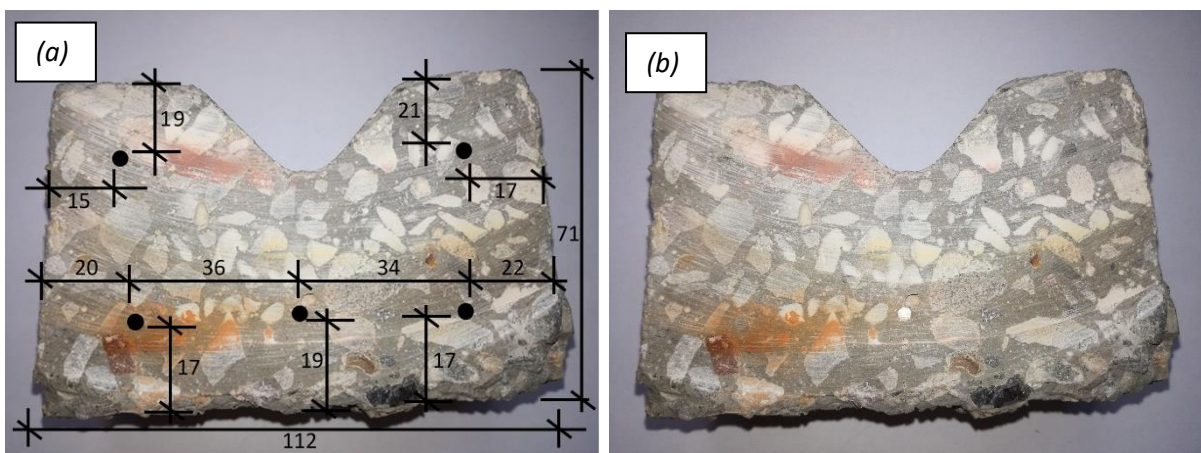


Figure 23. Photograph of (a) precast lintel cross section with dimension and (b) without dimensions.

The concrete bricks¹⁷ forming the masonry portion of the precast masonry lintel were standard concrete stock bricks with compressive strength of 7MPa and dimensions of 222mm in length, 106mm in width and 73mm in height.

The mortar used for the masonry works of the specimen had a mass mix ratio 1:3.2, PPC OPC CEM I 52,5 N to building sand. The average mortar strengths for the precast masonry lintel fire test specimens for tests 1, 2 and 3 were 149.06 kN, 124.8 kN and 92.3 kN, respectively. The loading rate of the mortar cube test was 150kN per minute. The aim was to conduct a fire test as soon as the mortar strength was equal to the 7MPa of the concrete bricks.

The composite lintels were built up and installed in the furnace using SANS10162 Part 1 as a guide. Referring to *Figure 24*, each of the three composite concrete lintels specimens were made up of two pre-stressed concrete lintels placed side by side with five courses of brick work above the lintel with a layer of mortar approximately 10mm thick between each brick

¹⁶ Purchased from Supreme Build It, Martindale.

¹⁷ Purchased from Builders Warehouse Strubens Valley, manufacturer unknown



course. The first course of brick placed on the lintel was a header course or English bond, this was to tie the two lintels together so that they would act dependently as one and to tie the two skins of brick together. Brick courses two, three, four and five, were ordinary staggered or stretcher courses. Double leaf brick-force was placed in the mortar between the lintel and the first course of bricks, as well as between the third and fourth courses of bricks.

The specimens were simply supported composite beam elements with a clear span of 2m and had a bearing area of 200mm by 200mm on either side. During casting, the specimen was propped on the centre of the span and mortar placed under the bearing positions on either side to allow for levelling of the precast masonry test specimen (Figure 24). The specimen was a composite double skin masonry beam.

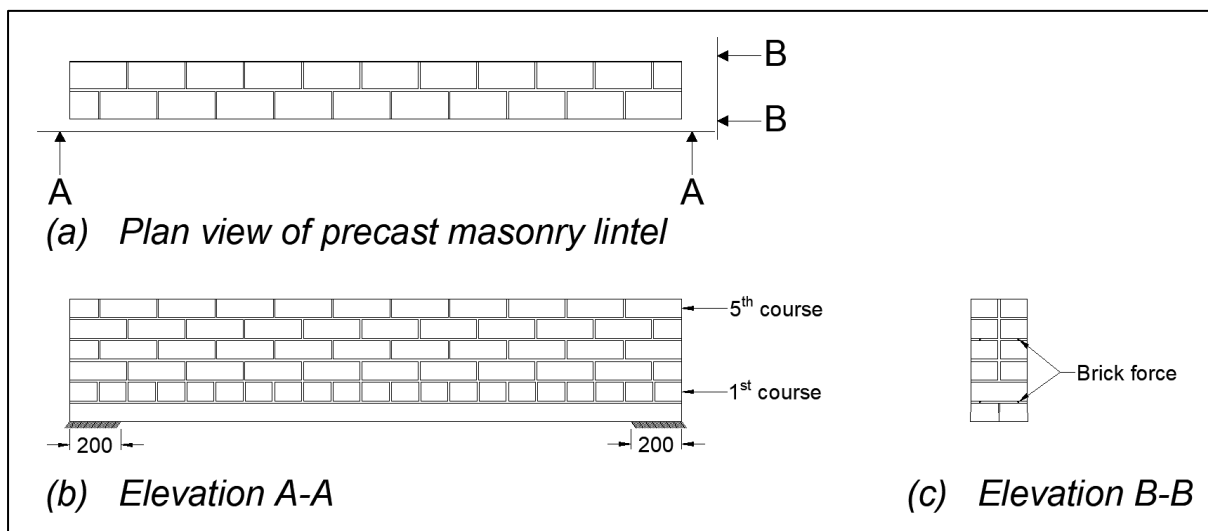


Figure 24. Precast composite masonry lintel fire test specimen schematic

4.3 Test procedure and monitoring

The specimens were exposed to fire on 3 sides: bottom, left and right. The top was not exposed to fire. Tolerance was created between the furnace and the composite lintel to allow for vertical displacement of the specimen and sealed with ceramic fibre blanket.

Test specimens 1 and 2 had no additional load applied during testing (Figure 25). Loading only occurred on test specimen three with a total load of 6.28 kN applied as a point load on the centre of the span of the specimen. The load was applied on a cross-sectional area of 220mm by 220mm (Figure 26 and Figure 27)

Temperatures were measured during the test with four type K thermocouples located on the top level of the specimen and furnace as per section 3.5. Temperatures were continuously



recorded every 2 seconds and regulated appropriately according to the standard time temperature curve. Visual observations were made on the behaviour of the specimen during and after each test.



Figure 25. Photograph of lintel test 1 with no load

A handwritten signature in black ink, consisting of several overlapping loops and a long horizontal stroke extending to the right.



Figure 26. Photograph of lintel test 3 with applied load before ignition



Figure 27. Photograph of lintel test with applied load during fire test

A handwritten signature or scribble in black ink, consisting of several overlapping loops and lines.

4.4 Results

To analyse the composite masonry lintel fire test results, the inspection took place approximately 24 hours after the fire tests, allowing enough time for the furnace to cool down (*Figure 28*). The results of the effect that the fire had on the specimens, can be seen in *Figure 29, 30 and 31* and are the results for composite masonry lintel fire tests 1, 2 and 3, respectively. The deflections of the concrete lintel were measured during the inspection.

In test 1, *Figure 29(a) to (f)*, only one lintel showed clear signs of delamination with a relative deflection of approximately 17mm from the brickwork on centre span. The 5 courses of brick work remained rigid, undeformed and undeflected in the vertical direction after exposure to the fire. The lintels, mortar and bricks also became brittle with signs of spalling on the lintels. The elasticity of the precast lintels had also greatly decreased. Many cracks were observed on the surface of the lintel especially between cement paste and aggregate. Test 1 was concluded after approximately 113 minutes of exposure to the standard time temperature curve.

In test 2, *Figure 30(a) to (d)*, both lintels showed clear signs of delamination with relative deflections between the top of the lintel and the bottom of the brick of approximately 9mm and 6mm for either side. The 5 courses of brick work remained rigid and undeformed after exposure to the fire. The lintels also became brittle with no clear signs of spalling, the elasticity of the lintels had also greatly decreased. Many fine cracks were observed on the surface of the lintel. Test 2 was concluded after approximately 91 minutes of exposure to the standard time temperature curve.

In test 3, *Figure 31(a) to (h)*, both lintels showed clear signs of delamination. The composite concrete lintel system had failed in terms of stability showing signs of excessive deformation of approximately 80mm in total. 60mm deflection is attributed to the additional load and self-weight and approximately 20mm to self-weight only. The specimen had not completely collapsed under its own self weight. The additional applied load only acted on the structure up to a deflection of approximately 60mm. It was observed that the bottom layer of brick force had snapped, but whether the strands in the precast lintel had also snapped is unclear. Many cracks were observed on the surface of the lintel. Test 3 was concluded after approximately 102 minutes of exposure to the standard time temperature curve.





Figure 28. Lintel in furnace approximately 24 hours post test

A handwritten signature or scribble in black ink, consisting of several overlapping loops and lines, located at the bottom center of the page.

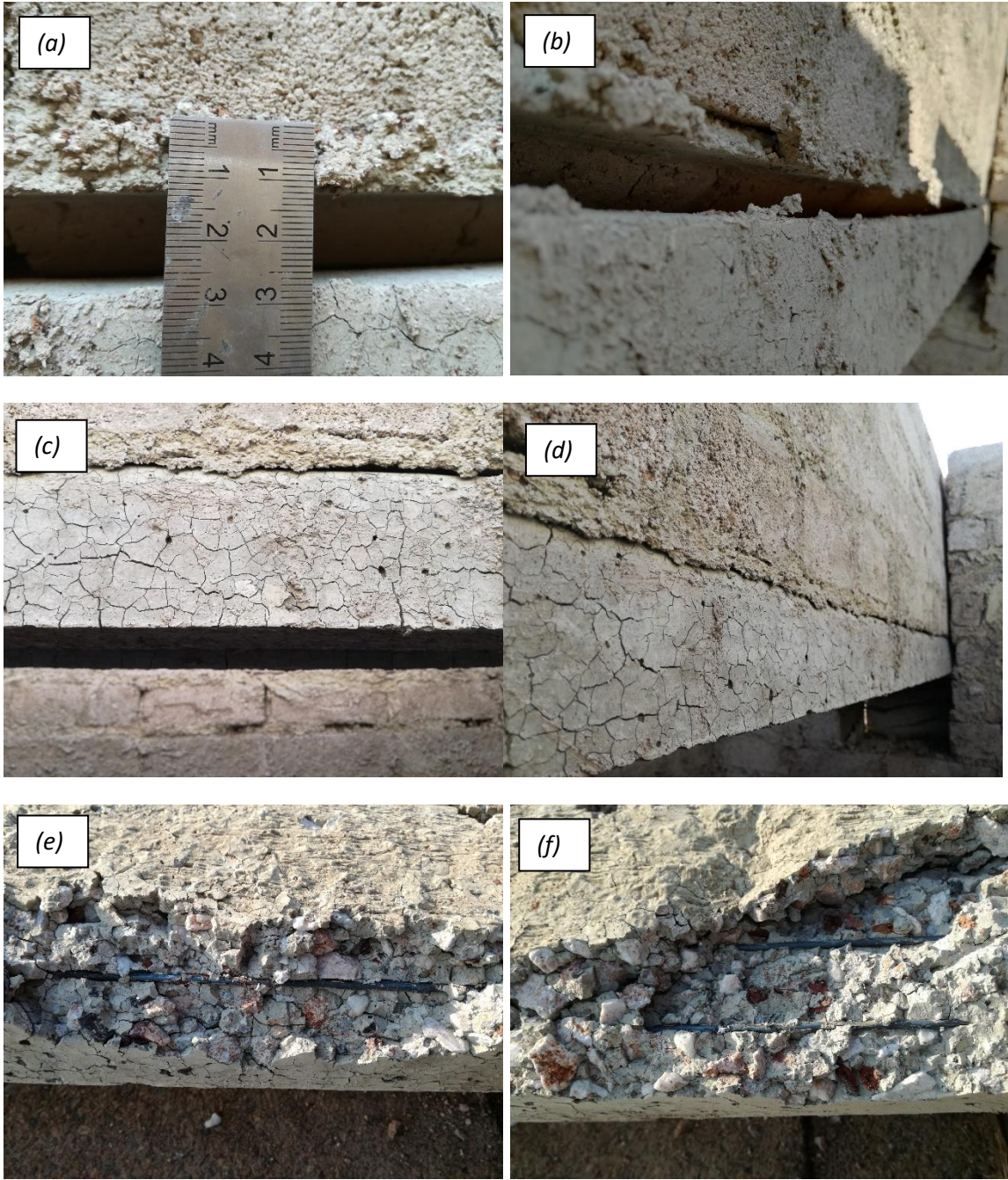


Figure 29. Lintel fire test 1 photographic results (a), (b), (c), (d), (e), and (f)

A handwritten signature in black ink, consisting of a stylized, cursive name.

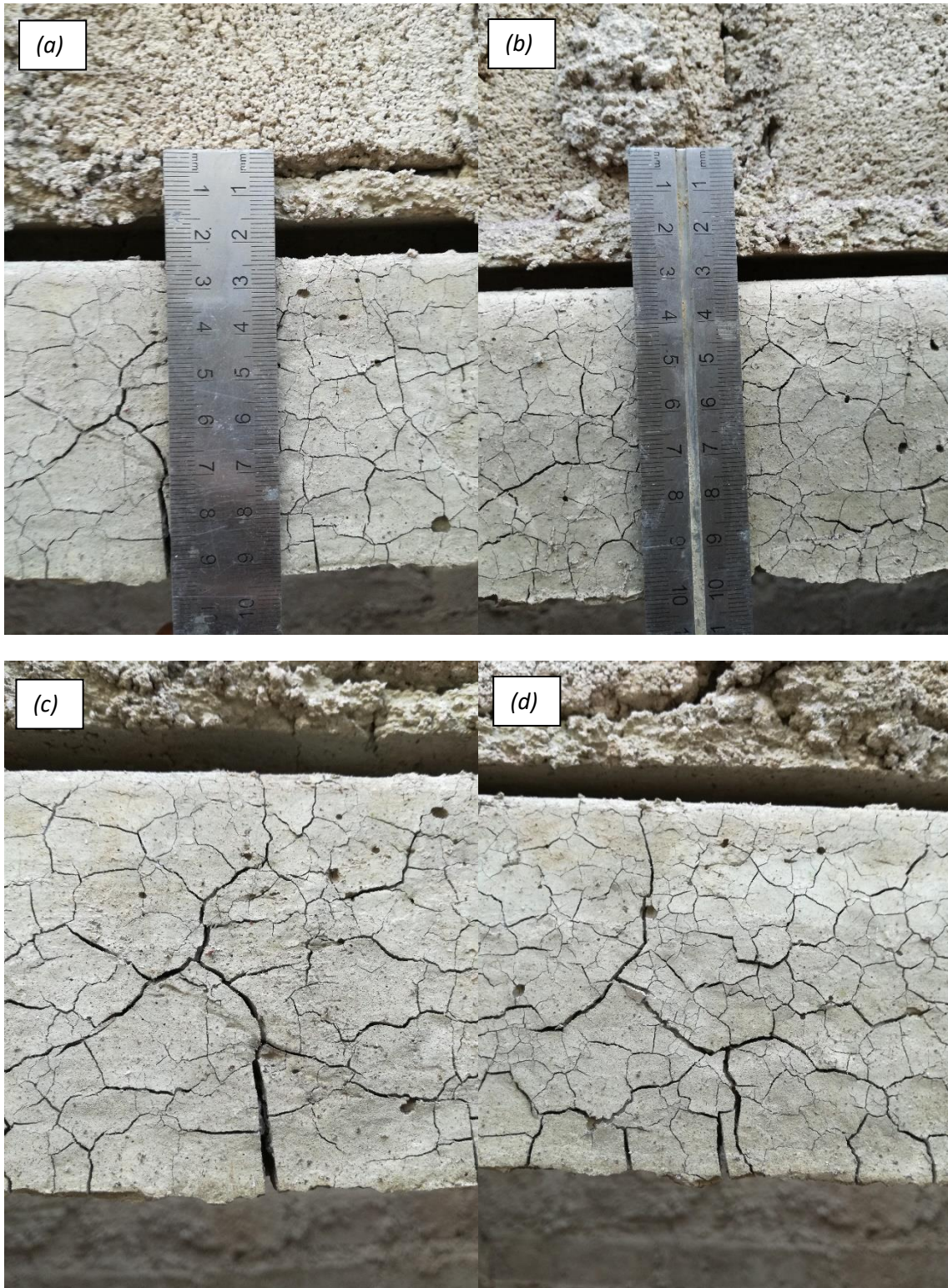


Figure 30. Lintel fire test 2 photographic results (a), (b), (c), and (d)

A handwritten signature or scribble, possibly a stylized name or initials, located at the bottom center of the page.



[Handwritten signature]

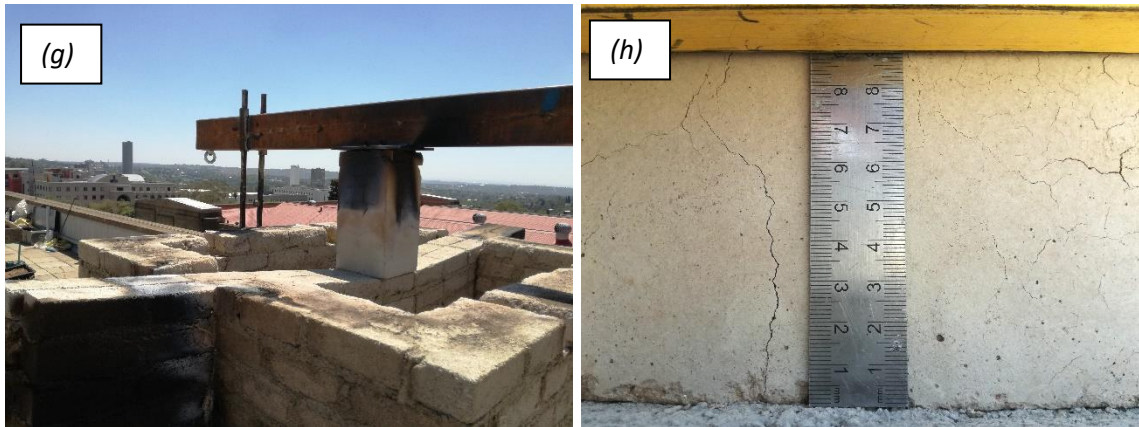


Figure 31. Lintel fire test 3 photographic results (a), (b), (c), (d), (e), (f), (g), and (h)

4.5 Discussion

In test specimens 1 and 2 the lintels delaminated from the brick work with the brickwork remaining intact and rigid and showing no signs of deflection under its own weight after being exposed to fire. Test specimen 3 collapsed under the applied load after being exposed to fire loading. In test 1 and 2 delamination and deflections of the lintels are due to only the self-weight of the concrete lintel acting in the vertical direction and the reduction of the material strength and the weakening of the physical properties of the concrete as well as the loss of tension in the steel strands due high temperatures. In the lintels, fine cracking can also be seen in the concrete especially around cement paste and aggregate interface, indicating a difference in the relative rates or degree in overall expansion of the aggregates and cement paste.

In all three tests the precast lintel and the masonry brick work do not maintain a bond and therefore do not act as a composite member after having been exposed to fire. The exposure to fire has greatly affected the bond between the precast lintel and the masonry brick work which is responsible for the shear transfer allowing the built-up specimen to act as a composite masonry lintel. This bond is completely removed by the exposure to fire and after the exposure to fire the composite masonry lintel can no longer be assessed as a composite member.

Figure 32 shows the moment of inertias for the individual cross sections of the components that make up the precast masonry lintel as well as the non-composite and composite masonry lintels. Assessing the composite masonry lintel as a composite member produces a moment of inertia of $8522 \times 10^5 \text{ mm}^4$, assessing it as non-composite member produces a moment of inertia of $3079 \times 10^5 \text{ mm}^4$. This equates to a 63% reduction in capacity after exposure to fire. It is for this reason that stirrups are an essential component for the transfer of shear.

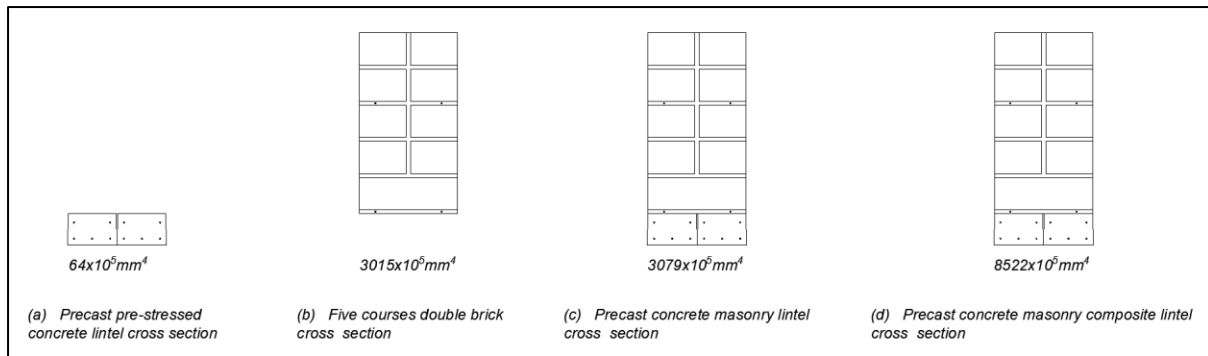


Figure 32. Cross sections analysed for second moment of inertia

5. Conclusion and recommendations for future studies

The thermocouple results obtained from tests 9, 10 and 11 demonstrate that the concept and design of the finite fuel furnace, with some modifications to ignition of the furnace, can be used for fire testing of horizontal load bearing structural and non-load bearing construction elements such as slabs, beams, and ceiling boards up to a maximum duration of 90 minutes in accordance with the standard time temperature curve defined by the SANS10177-2 Code of Practice.

From the three precast masonry lintel fire test results, it can be deduced that fire greatly reduces the bond between the lintel and brickwork responsible for horizontal shear transfer allowing the concrete lintel system to act a composite member. In this case the effect of no stirrups can easily be seen. This loss of bond reduces the moment capacity considerably and great care should be taken when designing a lintel masonry system as a composite member subject to fire. The testing also found that without any additional load the lintels act merely as formwork in the event of a 90-minute fire whereas the brick work can resist collapse under its own weight for a clear span of two meters.

It is recommended that future studies should move from a timber furnace to LPG furnace for three main reasons. The first reason being that the duration of a test can be increased without increasing the size of the furnace. Secondly, ignition, temperature control and regulation can be fine-tuned more easily to obtain better correlation between furnace temperatures and the standard time temperature curve. And finally, the smoke released from an LPG furnace would be much less and environmentally more acceptable.

Future studies should strive to achieve the 4-point loading and for greater data collection and adherence to codes of practice for certain aspects such as loading of specimens by means of incorporating load cell measurements, deflections measurements with LVDT's or by other means.

Future studies should ensure that technical furnace requirements such as number of thermocouples and thermocouple spacing are met. If additional investigation into lintels is conducted, these should be more representative of real-life elements and should be plastered.

Future testing of specimens should introduce control sample tests whereby the entire element is subject to fire loading and moment resistance capacities measured. Future studies should continue to further investigate moment resistance and consider investigating shear resistance, axial resistance and perhaps combinations of resistances. Eventually formulate a model whereby the full element in fire resistances can be calculated from the partial tests or equations or possibly tables could be compiled for beam element moment resistances in fire.

Acknowledgments

The author would like to sincerely thank Ms Nonhlanhla Mabusela from Timrite, Johan du Toit from Height Safety, Eddy Cik and Rob Ambrose from Cik Concrete, Trevor Hill from Flash Precast, Roy Smith from Mintroad Sawmills and RMS products for their donations towards this research. The author would like to sincerely thank his wife Victoria da Silva Pereira and friend Claudio Coito dos Santos for both helping and enduring this research, if it were not for you we would not be where we are now. The author would like to sincerely thank Professor Alex Elvin for having always been an incredible mentor.

A handwritten signature in black ink, consisting of several overlapping loops and a long horizontal stroke extending to the right.

References

- Abid, S.R. (2007). Effect of High Temperatures on Shear Transfer Strength of Concrete. *Journal of Engineering and Development*, 11(1).
- Alhawat, H., Hamid, R., Bahroom, S. and Mussa, M.H. (2019). Review on Large-Scale Fire Testing of Concrete Tunnel Lining. *Journal of Engineering and Applied Sciences*, 14(9), pp 2891-2887.
- Ambroziak, A., Kondrat, J. and Wesolowski, M. (2020). Shear resistance of low height precast concrete lintels. *Archives of Civil Engineering*, 66(3).
- Babrauskas, V. and Wickstrom, U. (1989). The Rational Development of Bench-scale Fire Tests for Full-scale Fire Prediction. *Fire Safety Science*, 2, pp. 813-822.
- Bezerra, A.C.S., Macie, I.P.S., Correa, E.C.S., Soares Junior, P.R.R., Aguilar, M.T.P. and Cetlin, P.R. (2019). Effect of High Temperature on the Mechanical Properties of Steel Fiber-Reinforced Concrete. *Fibers*, 7(12), pp. 100.
- Bjorge, J.S., Metallinou, M.M., Kraaijeveld, A. and Log, T. (2017). Small Scale Hydrocarbon Fire Test Concept. *Technologies*, 5 (4).
- Boissonnet, G., Bonnet, G. and Pedraza, F. (2019). Thermo-Physical Properties of HR3C and P92 Steels at High-Temperature. *Journal of Materials and Applications*, 8(2).
- Chen, H., Liu, G., Ren, J., Zhong, T. and Wang, M. (2018). Effect of High Temperature on the Bond Performance of Reinforcing Bars in Inorganic Polymer Concrete. *Journal of Advanced Concrete Technology*, 16, pp. 75-83.
- Dao, V., Torero, J., Ho, J., O'Moore, L., Maluk, C. and Bisby, L. (2016). Fire Performance of Concrete Using Novel Fire Testing Concrete. *Institute of Australia*, 42(1), pp.58-59.
- Department of Trade and Industry. (1990). *National Building Regulations No. R2378*.
- Department of Trade and Industry. (1977). *National Building Regulations and Building Standards Act: No.103 of 1977*.
- Di Maio, A., Giaccio, G. and Zerbino, R. (2002). Non-Destructive Tests for the Evaluation of Concrete Exposed to High Temperatures. *Cement, Concrete and Aggregates*, 24 (2).
- Dias, A.R.D.O., Amancio, F.A., Rafael, M.F.D.C. and Cabral, A.E.B. (2018). Study of propagation of ultrasonic pulses in concrete exposed at high temperatures. *Procedia Structural Integrity*, 11, pp. 84 -90.
- C, Black. (2018). *Fire testing methods of structural elements*. University of Witswatersrand.
- Husain, L.F. (2010). Residual Compressive and Flexural Strength of Self Compacting Concrete Exposed to High Temperature. *Journal of Engineering and Development*, 14 (1).
- Izzuddin, B.A. and Moore D.B. (2002). Lessons from a full-scale fire test. *Structures and Buildings*, 152(4), pp.319-329.
- Jansson, R. and Bostrom, L. (2011). Fire tests of loaded beams. In: *2nd International Workshop on Concrete Spalling due to Fire Exposure*. City: Delft.
- Jeronimo, V.A., Piccinini, A.C., Silva, B.V., Godinho, D.S.S., Bernardin, A.M. and Vargas, A. (2020). Influence of concrete admixture on the bond strength of reinforced concrete submitted to high temperature. *Ibracon Structures and Materials Journal*, 13 (2), pp. 212 – 221.
- Kwon, K. and Kweon, O. (2019). Time-temperature Analysis of High-strength Concrete Exposed to High Temperatures. *Journal of the Korean Society of Hazard Mitigation*, 18 (7), pp.227-232.
- Lim, L. and Wade, C. (2012). *Experimental Fire Tests of Two-Way Concrete Slabs*. University of Canterbury.



- Lima, R.C.A., Haesbaert, F.M., Caetano, L.F., Bergmann, C.P. and Silva Filho, L.C.P. (2005). Microstructural changes in high density concretes exposed to high temperatures. *Ibracon Materials Journal*, 1(1) pp.7 -14.
- Miah, M.J. (2015). Behaviour of Concrete at High Temperature, [online]. Available from: https://www.researchgate.net/publication/329987167_Behaviour_of_Concrete_at_High_Temperature. [Accessed 2 July 2020].
- Pamu, P. and Rekha, K. (2018). Performance of Ternary Blended Concrete Exposed to High Temperatures International. *Journal of Latest Engineering and Management Research*, 3 (7) pp. 57-62.
- Radzi, N.A.M., Hamid, R. and Mutalib, A.A. (2016). A Review of Methods, Issues and Challenges of Small-scale Fire Testing of Tunnel Lining Concrete. *Journal of Applied Science*, 16, pp.293-301.
- Ren, F. and Xiaoying, T. (2019). Mechanical properties of Grade 91 steel at high temperatures. *Journal of Physics: Conference Series*.
- SANS 10100-1. (2000). *The structural use of concrete, Part 1: Design*, ed., 2.02. Pretoria: South African Bureau of Standards.
- SANS 10100-2:2014. (2014). *The structural use of concrete, Part 2: Materials and execution of work*, ed. 3.00. Pretoria: South African Bureau of Standards.
- SANS 10164-1. (1980). *The structural use of masonry, Part 1: Unreinforced masonry walling*, ed. 1. Pretoria: South African Bureau of Standards.
- SANS 10164-2. (2008). *The structural use of masonry, Part 2: Structural design and requirements for reinforced and pre-stressed masonry*, ed. 1.02. Pretoria: South African Bureau of Standards.
- SANS 10177-1. (2005). *Fire testing of materials, components and elements used in buildings, Part 1: General introduction to the methods of test*, ed. 1.1. Pretoria: South African Bureau of Standards.
- SANS 10177-10. (2007). *Fire testing of materials, components and elements used in buildings, Part 10: Surface burning characteristics of building materials using the inverted channel tunnel test*, ed. 1.01. Pretoria: South African Bureau of Standards.
- SANS 10177-11. (2007). *Fire testing of materials, components and elements used in buildings, Part 11: Large-scale fire performance evaluation of building envelope thermal insulation systems (with or without sprinklers)*, ed. 1.01. Pretoria: South African Bureau of Standards.
- SANS 10177-12. (2014). *Fire testing of materials, components and elements used in buildings, Part 12: Test methods for fire tests of roof coverings*, ed. 1.00. Pretoria: South African Bureau of Standards.
- SANS 10177-2. (2005). *Fire testing of materials, components and elements used in buildings, Part 2: Fire resistance test for building elements*, ed. 1.1. Pretoria: South African Bureau of Standards.
- SANS 10177-3. (2005). *Fire-testing of materials, components and elements used in buildings Part 3: Surface fire index of finishing materials*, ed. 1.02. Pretoria: South African Bureau of Standards
- SANS 10177-4. (2005). *Fire testing of materials, components and elements used in buildings, Part 4: Surface fire index of floor coverings*, ed. 1.03. Pretoria: South African Bureau of Standards.
- SANS 10177-5. (2012). *Fire testing of materials, components and elements used in buildings, Part 5: Non-combustibility at 750 °C of building materials*, ed. 1.02. Pretoria: South African Bureau of Standards.



- SANS 10177-6. (2005). *Fire testing of materials, components and elements used in buildings, Part 6: Non-combustibility at 300 °C of electrical insulation materials*, ed. 1.01. Pretoria: South African Bureau of Standards.
- SANS 10177-7. (2005). *Fire testing of materials, components and elements used in buildings, Part 7: Fire test for fire-check properties of building elements*, ed. 1.01. Pretoria: South African Bureau of Standards
- SANS 10177-8. (2006). *Fire testing of materials, components and elements used in buildings, Part 8: Surface burning characteristics of building materials*, ed. 1.00. Pretoria: South African Bureau of Standards.
- SANS 10177-9. (2006). *Fire testing of materials, components and elements used in buildings, Part 9: Small-scale burning characteristics of building materials: ignition, flame spread and heat contribution*, ed. 1.00. Pretoria: South African Bureau of Standards.
- SANS 10400-A. (2010). *The application of the National Building Regulations, Part A: General principles and requirements*, ed. 3. Pretoria: South African Bureau of Standards.
- SANS 10400-T. (2011). *The application of the National Building Regulations, Part T: Fire protection*, ed. 4. Pretoria: South African Bureau of Standards.
- SANS 1504. (2015). *Pre-stressed concrete lintels*, ed.2.00. Pretoria: South African Bureau of Standards.
- SANS 282. (2004). *Bending dimensions and scheduling of steel reinforcement for concrete*, ed. 5.1. Pretoria: South African Bureau of Standards.
- Setiyarto Y.D. and Fira H.Y (2019). Behaviour of Concrete Burned with High Temperature. *IOP Conference Series: Materials Science and Engineering*, 662.
- Sumathipala, K, Carpenter, D.W., Monette, R.C., Seguin, Y.P. and Loughheed, G.D. (2001). Small-Scale and Full-Scale Fire Tests of Four Construction Materials. *National Research Council Canada: Institute for Research in Construction*.
- Topcu, I.B. and Karakurt, C. (2008). Properties of Reinforced Concrete Steel Rebars Exposed to High Temperatures. *Research Letters in Materials Science*.
- Torres, A., Ramos-Canon, A., Prada-Sarmiento, F. and Botia-Diaz, M. (2016). Mechanical behaviour of concrete cold joints. *Revista Ingenieria de Construccion*, 31 (3), pp.151-162.
- Varona, F.B., Baeza, F.J., Ivorra, S. and Bru, D. (2011). Experimental analysis of the loss of bond between rebars and concrete exposed to high temperatures. *Dyna (Bilbao)*, 90, pp. 78-86.
- Wald, F., Simoes, da Silva, L., Moore, D.B. and Lennon, T. Structural integrity fire test, [online]. Available from: [[http://people.fsv.cvut.cz/~wald/Clanky%20v%20Adobe%20\(Pdf\)/Copenhagen_5_Text_Wald-Silva-Moor-Lennon.pdf](http://people.fsv.cvut.cz/~wald/Clanky%20v%20Adobe%20(Pdf)/Copenhagen_5_Text_Wald-Silva-Moor-Lennon.pdf)]. [Accessed 2 July 2020].
- Wegrzynski, W. and Turkowski, P. (2018). Material properties and the energy balance in standardized fire testing. *MATEC Web of Conferences*.
- Westhuyzen, S.V.D., Walls, R., Koker, N.D. (2020). Fire tests of South African cross-laminated timber wall panels, fire ratings, charring rates, and delamination. *Journal of the South African Institute of Civil Engineering*, 62 (1), pp. 33 -41.
- Willson, M. (2020). Are Small-scale Fire Tests Adequate. *The Catalyst, JOIFF*.
- Yuzer, N., Akbas B. and Kizilkanat, A.B. (2007). Predicting the Compressive Strength of Concrete Exposed to High Temperatures with a Neural Network Model. In: *Turkish Cement Manufacturers Association, 3rd International Symposium, Sustainability in Cement and Concrete*. At: Istanbul.

